Mammalian Abp1, a Signal-responsive F-Actin–binding Protein, Links the Actin Cytoskeleton to Endocytosis Via the GTPase Dynamin

Michael M. Kessels,* Åsa E.Y. Engqvist-Goldstein,‡ David G. Drubin,‡ and Britta Qualmann*

*Department of Neurochemistry and Molecular Biology, Leibniz Institute for Neurobiology, D-39008 Magdeburg, Germany; and ‡Department of Molecular and Cell Biology, University of California, Berkeley, California 94720-3202

Abstract. The actin cytoskeleton has been implicated in endocytosis, yet few molecular links to the endocytic machinery have been established. Here we show that the mammalian F-actin–binding protein Abp1 (SH3P7/HIP-55) can functionally link the actin cytoskeleton to dynamin, a GTPase that functions in endocytosis. Abp1 binds directly to dynamin in vitro through its SH3 domain. Coimmunoprecipitation and colocalization studies demonstrated the in vivo relevance of this interaction. In neurons, mammalian Abp1 and dynamin colocalized at actin-rich sites proximal to the cell body during synaptogenesis. In fibroblasts, mAbp1 appeared at dynamin-rich sites of endocytosis upon growth factor stimulation. To test whether Abp1 functions in endocytosis, we overexpressed several Abp1 constructs in Cos-7 cells and assayed receptor-mediated endocytosis. While overexpression of Abp1's actin-binding modules did not interfere with endocytosis, overexpression of the SH3 domain led to a potent block of transferrin uptake. This implicates the Abp1/dynamin interaction in endocytic function. The endocytosis block was rescued by cooverexpression of dynamin. Since the addition of the actin-binding modules of Abp1 to the SH3 domain construct also fully restored endocytosis, Abp1 may support endocytosis by combining its SH3 domain interactions with cytoskeletal functions in response to signaling cascades converging on this linker protein.

Key words: actin cytoskeleton • dynamin • endocytosis • SH3P7 • neuronal plasticity

Introduction

Dynamic regulation of the actin cytoskeleton is crucial for many cellular functions. In yeast, a functional connection between the cortical actin cytoskeleton and endocytosis exists. Mutations in several actin-binding proteins and even in actin itself result in endocytosis defects (for review, see Geli and Riezman, 1998; Wendland et al., 1998). The molecular basis for these effects is not understood. However, genetic studies using actin and cofilin mutants suggest that rapid turnover of the cortical actin cytoskeleton is required for endocytic internalization. In mammals, such a connection between cytoskeletal and endocytic functions has not been as clearly established. The use of drugs such as cytochalasins, latrunculins, and jasplakinolide or mutant forms of the Rho family of small GTPases to perturb the actin cytoskeleton (reviewed by Ellis and Mellor, 2000) often yields inconsistent results when different assays and cell systems are used, as shown by a broad study by Fujimoto et al. (2000, and references therein).

The endocytic uptake of extracellular medium and plasma membrane is accomplished by several distinct pathways, and requires a coordinated interaction of the components of the endocytic machinery (reviewed by Brodin et al., 2000). The fission reaction, which gives rise to endocytic vesicles pinched off from the plasma membrane, is controlled by the large GTPase dynamin (for review, see Sever et al., 2000). A rapidly growing list of Src homology 3 (SH3)[1] domain-containing accessory proteins is also implicated in the formation of endocytic vesicles. These include amphiphysins (reviewed in Wigge and McMahon, 1998), endophilins (Micheva et al., 1997; Ringstad et al., 1997), DAP160/intersectin scaffolding proteins (Roos and Kelly, 1998; Yamabhai et al., 1998), and syndapins (Qualmann et al., 1999). These proteins can form stable complexes with the COOH-terminal proline-rich domain of dynamin. SH3 domain–proline-rich domain interactions have been demonstrated to strongly activate dynamin's GTPase activity (Gout et al., 1993). Little, however, is known about the

Address correspondence to Michael M. Kessels, Department of Neurochemistry and Molecular Biology, Leibniz Institute for Neurobiology, Postfach 1860, D-39008 Magdeburg, Germany. Tel.: 49 391 6263 225. Fax: 49 391 6263 229. E-mail: kessels@ifn-magdeburg.de

[1]*Abbreviations used in this paper:* ADF-H, actin-depolymerizing factor homology; GFP, green fluorescent protein; GST, glutathione-S-transferase; HA, hemagglutinin; HEK, human endothelial kidney; SH3, Src homology 3.

potential cross talk between the endocytosis machinery and the cortical cytoskeleton.

Recently, a few candidates for proteins that could function at the interface between actin and endocytosis in mammalian cells have emerged (for review, see Qualmann et al., 2000). Syndapins are the potential molecular links that have been most extensively characterized functionally. Syndapins, which bind to both dynamin and to N-WASP (Qualmann et al., 1999), are implicated in endocytic function by both in vitro reconstitution and in vivo studies (Simpson et al., 1999; Qualmann and Kelly, 2000). They are also capable of promoting actin polymerization through a mechanism involving the Arp2/3 complex (Qualmann and Kelly, 2000). Another candidate is profilin, a nucleotide exchange factor for monomeric actin. Profilin has been found to bind to dynamin as well (Witke et al., 1998).

Elucidation of the role of the actin cytoskeleton in endocytosis in mammals would result if it were possible to identify the molecular links at the interface of actin and endocytosis and to unravel their functions. One approach is to search for mammalian homologues of yeast cytoskeletal proteins genetically implicated in endocytosis. We previously described two such putative homologues. First, the mouse protein mHip1R (Huntingtin-interacting protein 1–related), which is related to Sla2p (synthetic lethal with Abp1) (Holtzman et al., 1993), also named End4 (Raths et al., 1993). Hip1R is a novel actin-binding component of the clathrin coat (Engqvist-Goldstein et al., 1999). The second protein, mAbp1 (Lappalainen et al., 1998; Kessels et al. 2000), is the mouse homologue of yeast Abp1 (actin-binding protein 1; Drubin et al., 1988). This protein was also systematically named SH3P7 because it was identified in a screen for SH3 domain–containing proteins (Sparks et al., 1996). The ubiquitously expressed 56-kD protein mAbp1 contains two independent F-actin binding modules, one is the NH2-terminal actin-depolymerizing factor homology (ADF-H) domain and the other the central helical domain. Mammalian Abp1 is specifically recruited to dynamic actin structures (Kessels et al., 2000). This localization is somewhat reminiscent of the localization of the yeast protein, which is found in cortical actin patches accumulating in the yeast bud but not at actin cables (Drubin et al., 1988). This selectivity for sites of high actin dynamics manifests in a strong accumulation at the leading edge of moving and of spreading cells, whereas in resting cells Abp1 shows a more uniformly distributed, punctate immunostaining pattern. The shift to the periphery is controlled by signal transduction pathways leading to activation of the GTPase Rac1 and can be directly induced by a dominant-active mutant version of Rac1 (Kessels et al., 2000). Several signaling pathways may converge on Abp1, as Abp1 proteins from different species were found to interact with (a) Src kinases (SH3P7; Lock et al., 1998), (b) the hematopoietic progenitor kinase 1 (HIP-55; Ensenat et al., 1999), and (c) the myosin I heavy chain kinase (DdAbp1; de la Roche and Cote, 1999).

Here we report that Abp1 can interact with the GTPase dynamin in vitro and in vivo and may be involved in membrane transport processes in neuronal and nonneuronal cells. We demonstrate that overexpression of the Abp1 SH3 domain blocks endocytosis in vivo and that the stepwise readdition of the actin-binding modules of Abp1 restores endocytic function. Our analysis suggests that Abp1 is a functional and physical link between the cortical actin cytoskeleton and endocytosis on which several signaling pathways converge.

Materials and Methods

DNA Constructs and Recombinant Proteins

The majority of glutathione-S-transferase (GST)–mAbp1 fusion plasmids used in this study for expression in bacteria were described previously (Kessels et al., 2000). Further GST-fusion constructs, pGAT2-mAbp1 (1–370; ADF-H/hel/flex) and pGAT2-mAbp1 (282–433$^{P422L,\ G425R}$; flex/SH3^{mut}) were generated accordingly. The construct containing two point mutations within the SH3 domain of mouse Abp1 (P422L and G425R) was generated by PCR with a reverse primer giving rise to these amino acid exchanges. All constructs were sequenced to ensure that no undesired mutations were introduced. To generate NH_2-terminally myc-tagged Abp1 constructs for overexpression in mammalian cells, the mouse Abp1 sequences were subcloned into the pRK5 vector (provided by Alan Hall, University College London, London, UK). The myc-tagged overexpression construct containing the NH_2-terminal SH3 domain of Grb2 was generated by subcloning from Grb2N-pGEX2T (provided by Brian Kay, University of Wisconsin-Madison, Madison, WI) into pRK5. Flag-Abp1 was generated by subcloning full-length Abp1 from pGAT2 into the pCMV-Tag2B vector (Stratagene).

The rat endophilin SH3 domain was cloned from a rat brain cDNA library (MATCHMAKER in pGAD10; CLONTECH Laboratories, Inc.) by PCR and cloned into pGEX-2T. Sequencing confirmed that the sequence was identical to the partial rat endophilin clone AF96003 in GenBank.

Dynamin2aa–green fluorescent protein (GFP) was kindly provided by Marc McNiven (Mayo Clinic and Foundation, Rochester, MN) and HA-dynamin1 constructs were provided by Sandra L. Schmid (Scripps Research Institute, La Jolla, CA).

GST-fusion proteins were expressed in *Escherichia coli* BL21 cells and purified using glutathione agarose beads (Sigma-Aldrich), as described previously (Kessels et al., 2000), and dialyzed. GST fusion proteins comprising the syndapin I SH3 and syndapin I SH3^{P434L} were described by Qualmann et al. (1999) and prepared accordingly.

Tissue Homogenates and Cell Extracts

Postnuclear supernatants from different rat and mouse tissues were prepared and processed for Western blotting as described (Qualmann et al., 1999; Kessels et al., 2000).

Homogenates of Cos-7 and HeLa cells overexpressing myc-Abp1 fusion proteins were prepared from high-density cultures in six-well plates 24–48 h after transfection. Cells were harvested and resuspended in 30 μl lysis buffer [1% Triton X-100 in PBS supplemented with protease inhibitors (complete protease inhibitor tablet, EDTA-free; Roche)] and incubated for 20 min on ice. The samples were then spun for 20 min at 14,000 *g* at 4°C. Supernatants were separated on 5–20% SDS-PAGE, and immunoblotted with anti–myc antibody.

Blot Overlay Analysis and Coprecipitation Assays

Blot overlays using recombinant GST-Abp1 fusion proteins were performed according to Roos and Kelly (1998). Coprecipitations of proteins interacting with GST-fusion proteins of Abp1 were performed with 0.625 mg rat brain extract according to Qualmann et al. (1999). Bound proteins were separated on 4–15% gradient SDS-PAGE, blotted to nitrocellulose, and probed for with various antibodies. Dynamin was detected by the monoclonal antibody Hudy1, synapsin 1a/b were detected with a monoclonal anti–synapsin 1 antibody (Synaptic Systems GmbH) or a rabbit anti–synapsin 1 antibody (Biogenesis), synaptojanin was detected by a polyclonal rabbit anti–synaptojanin antibody (provided by Peter McPherson, McGill University, Montreal, Quebec, Canada), and actin was detected using the monoclonal antibody C4 (ICN Biomedicals).

Immunoprecipitations

Complete rat brains were prepared from 8-wk-old male rats. The brains were frozen immediately in liquid nitrogen. Dissected rat brains were homogenized 1:3 (wt:vol) in 10 mM Hepes, 1 mM EGTA, 10 mM NaCl, 0.1 mM $MgCl_2$, pH 7.4, supplemented with protease inhibitors (see above)

with an ultra turrax at 20,000 rpm for 10 s and centrifuged at 150,000 *g* for 45 min. Triton X-100 (1% final) and NaCl (25 mM final) were added to the supernatant. Affinity-purified anti–mAbp1 antibodies (GP5; Kessels et al., 2000) or unrelated guinea pig IgGs were immobilized on protein G sepharose (Amersham Pharmacia Biotech) in the presence of 5% BSA. After several washes with IP buffer (10 mM Hepes, pH 7.4, 1 mM EGTA, 0.1 mM $MgCl_2$, 25 mM NaCl, 1% Triton X-100), the resin was incubated with 1 mg rat brain high speed supernatant overnight at 4°C. Beads were washed four times with IP buffer. Bound proteins were eluted with SDS sample buffer. All procedures were carried out at 4°C. Eluates were separated on 8% SDS-PAGE and analyzed by immunoblotting using monoclonal anti–dynamin antibodies (Transduction Laboratories).

Dynamin was immunoprecipitated from brain high speed supernatant (prepared as above) in IP buffer (100 or 150 mM NaCl final) with the monoclonal antibody Hudy1 (Upstate Biotechnology) prebound to protein G sepharose.

For immunoprecipitations of epitope-tagged proteins, human endothelial kidney (HEK) cells transfected with Flag-Abp1 and Dynamin2aa-GFP DNA constructs were grown for another 2 d, harvested, and homogenized in IP buffer (100 mM NaCl final) for 20 min at 4°C. 6 μg monoclonal anti–Flag antibody M2 (Sigma-Aldrich) or nonimmune mouse IgG (Santa Cruz Biotechnology, Inc.) bound to protein G Sepharose were incubated with the high speed supernatants prepared from the lysed HEK cells overnight at 4°C. The precipitated material was washed and probed for coprecipitated proteins by SDS-PAGE and immunoblotting using rabbit anti–Flag antibodies (Zymed Laboratories) and monoclonal anti–GFP antibodies (Babco).

Cell Culture and Immunofluorescence Microscopy

Primary hippocampal cultures were prepared and grown on poly-D-lysine–coated glass coverslips according to Goslin and Banker (1991). HEK293, Cos-7, and NIH3T3 cells were maintained in Dulbecco's modified Eagle's medium containing 10% fetal bovine serum.

Serum-starved NIH3T3 fibroblasts were activated by replating the cells onto fibronectin-coated coverslips. Further activation of signaling cascades leading to Rac1 activation and lamellipodia formation was achieved by addition of 300 ng/ml PMA (Sigma-Aldrich) and 5 ng/ml human recombinant PDGF (Sigma-Aldrich). The cells were incubated with PMA and PDGF for 10 min, washed with warm PBS, and then either perforated with ice-cold 0.02% saponin (Sigma-Aldrich) for 10 s or directly fixed with 4% paraformaldehyde in PBS, pH 7.4, containing 0.9 mM $CaCl_2$ and 0.5 mM $MgCl_2$ for 20 min.

Primary hippocampal neurons were fixed in 4% paraformaldehyde for 15 min at room temperature. After an incubation with 25 mM glycine in PBS for 15 min, cells were permeabilized and blocked for 1 h in 2% BSA, 10% horse serum, and 0.02% saponin in PBS (block solution). Incubations with antibodies were performed according to Kessels et al. (2000). As primary antibodies, affinity-purified polyclonal anti–mAbp1 guinea pig antibody GP5 (Kessels et al., 2000), monoclonal anti–dynamin antibody Hudy1 (Upstate Biotechnology), affinity-purified polyclonal anti–HIP1R guinea pig antibody GP#8 (Engqvist-Goldstein et al., 1999), monoclonal anti–AP2 antibody (Oncogene Research Products), polyclonal anti–Eps15 rabbit antibody #896 (Santa Cruz Biotechnology, Inc.), monoclonal anti–Flag antibody M2 (Sigma-Aldrich), monoclonal anti–HA antibody HA.11 (BabCO), polyclonal anti–myc rabbit antibody (Santa Cruz Biotechnology, Inc.), and monoclonal anti–myc antibody 9E10 (BAbCO) were used.

Secondary antibodies used in this study include FITC goat anti–guinea pig (ICN Biomedicals), rhodamine goat anti–guinea pig (ICN Biomedicals), Alexa Fluor™ 568 goat anti–mouse (Molecular Probes), rhodamine donkey anti–mouse (Jackson ImmunoResearch Laboratories), FITC donkey anti–mouse (Jackson ImmunoResearch Laboratories), Alexa Fluor™ 568 goat anti–rabbit (Molecular Probes) and Alexa Fluor™ 488 goat anti–rabbit (Molecular Probes). F-actin was stained with Texas red-phalloidin (Molecular Probes) at 1:300.

Cells were viewed using an inverted Eclips TE300 fluorescence microscope (Nikon), a DMRD fluorescence microscope (Leica), or a TCS NT laser confocal microscope with a TCS software package (Leica). Images were recorded digitally and processed using Adobe Photoshop software.

Transferrin Uptake Assays

Cos-7 cells were plated onto glass coverslips and transfected with different myc-tagged constructs using the LipofectAMINE PLUS transfection reagent method according to the instructions of the manufacturer (GIBCO BRL). Transferrin uptake assays were performed 48 h after transfection as described previously (Kessels et al., 2000; Qualmann and Kelly, 2000). The percentages of transfected cells showing no detectable uptake of transferrin significantly reduced transferrin signals, and normal levels of internalized transferrin were calculated by scoring and counting cells in several independent experiments. Two categories, high- and low-expressing cells, were scored independently to obtain higher similarities of expression levels within the groups and thus a better comparability between individual transfected cells. Data of individual assays were subsequently averaged and the standard deviations calculated. All graphs depicted represent data obtained upon quantification of endocytosis of the group of transfected cells expressing higher levels of epitope-tagged proteins.

For the rescue experiments, cells were double transfected with Abp1 constructs and hemagglutinin (HA)-dynamin1. Due to the lower expression rates of the Abp1 constructs (data not shown), immunostainings for those and not for dynamin were used in the endocytosis quantifications. To compare the endocytosis data obtained with the value of the theoretically achievable maximal rescue, double labelings of both epitope tags were performed and the rates of cotransfection were determined in parallel to the endocytosis assays.

Results

Identification of Binding Partners of the Abp1 SH3 Domain

To gain further insights into the functions of mammalian Abp1, which binds to F-actin via two NH_2-terminal domains, we attempted to identify interaction partners of the two COOH-terminal domains of this protein. We searched for direct binding partners in a variety of rat tissues using a blot overlay technique (Fig. 1, a and b). Several bands were detected using the COOH-terminal half of Abp1 as a probe (Fig. 1 a). The most prominent bands were detected in brain (a weak band at ~60 kD, a double band at 75/80 kD, and bands at 100, 145, and 180 kD). Proteins were also detected in testis (a weak band at 60 kD and a doublet of 100 and 105 kD) (Fig. 1 a). In the other tissues, the intensities of bands were much lower. A blot overlay using the NH_2-terminal half of the protein containing the two F-actin–binding modules did not reveal any bands (data not shown). Using a GST fusion protein of the SH3 domain alone, we were able to show that the interactions detected were due to the COOH-terminal SH3 domain and not the flexible domain, which was also contained in the original fusion construct (Fig. 1 b). In general, the signal intensities were slightly higher using the SH3 domain alone compared with the COOH-terminal half of Abp1. This may be due to the fact that the flexible domain is sensitive to proteolytic degradation (Kessels et al., 2000); such cleavages would result in loss of GST detection. These experiments also showed that the binding specificities of the SH3 domain were not affected by the presence or absence of neighboring sequences.

The pattern of bands detected was very suggestive of their identity because SH3 domains of proteins with close homology to the Abp1 SH3 domain (i.e., those of syndapins and endophilins) also detected bands of similar sizes (Micheva et al., 1997; Qualmann et al., 1999). To identify the binding partners detected in the blot overlay studies, we performed affinity purifications using rat brain extracts and a GST-Abp1 SH3 domain fusion protein immobilized on glutathione sepharose. Bound proteins were eluted and assayed via immunoblotting (Fig. 1 c). Parallel incubations were performed using equal amounts of the SH3 domains of endophilin 1 and syndapin I to detect interacting proteins and additionally to compare the apparent affinities

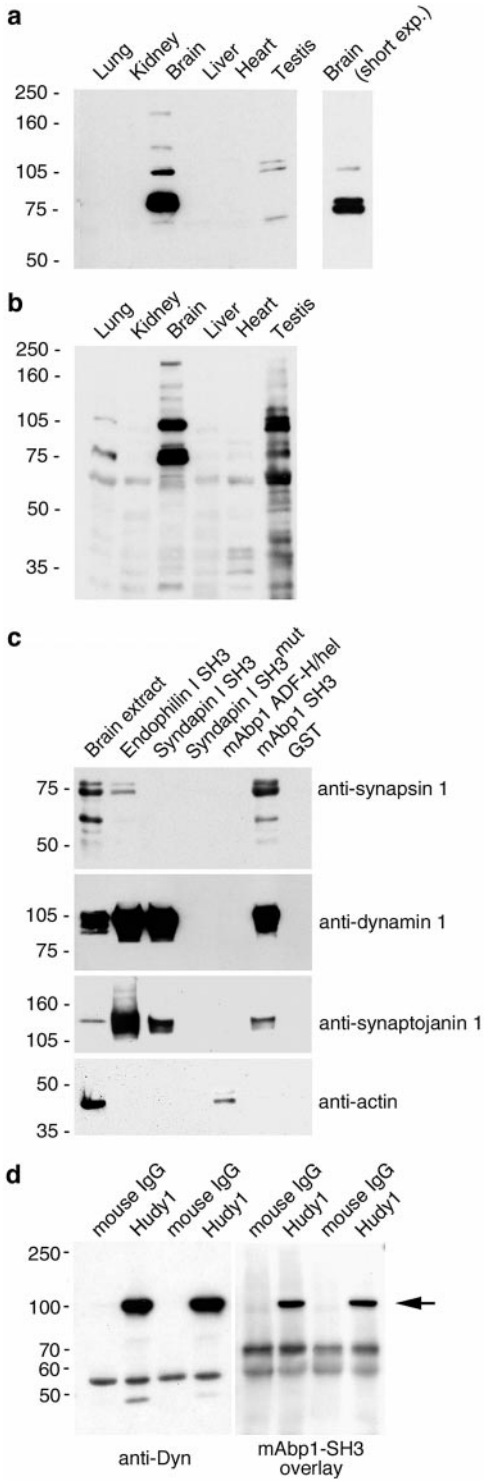

Figure 1. Identification of proteins interacting with the SH3 domain of Abp1. (a) Blot overlay analysis using a GST-fusion protein containing the COOH-terminal half of Abp1 onto different rat tissue homogenates identified several bands prominent in brain at 75/80, 100, 145, and 180 kD. (b) Blot overlay analysis using a GST-fusion protein of the SH3 domain revealed bands of similar molecular weights not only in brain but in part also in testis and lung. (c) Affinity purifications of proteins interacting with the SH3 domains of Abp1, endophilin I, and syndapin I. Equal amounts of fusion proteins and brain extracts (0.625 mg brain protein per pull down) were used. 12.45 μg of starting material (corresponding to 1/50) were loaded for comparison. (d) Immunoprecipitated dynamin (arrow) was detected by both antidynamin antibodies (left) and by the Abp1-SH3 domain (right). Left two lanes in each gel: IP buffer with 150 mM salt; right two lanes in each gel: IP buffer with 100 mM salt.

by which ligands are bound by Abp1, syndapin, and endophilin SH3 domains in vitro. The strength of the interactions in vitro may provide hints to the relevance of the observed associations.

Immunoblotting for synapsin 1, a synaptic vesicle protein, which is proposed to anchor the reserve pool of synaptic vesicles via binding to actin (reviewed in Hilfiker et al., 1999), revealed an intense double band of 75/80 kD as well as some degradation products, the most prominent of which was detected at 60 kD. Synapsin 1 was strongly bound by the Abp1 SH3 domain, whereas bindings to endophilin 1 and syndapin I SH3 domains were weaker and required longer exposure times for detection (Fig. 1 c). Dynamin1 was also precipitated. The GTPase dynamin, which runs with an apparent molecular weight of ~100 kD, and isoforms of which are abundant in brain and testis, was found to be strongly bound in affinity purifications with all three SH3 domains (Fig. 1 c). Synaptojanin 1 (McPherson et al., 1994), detected as a faint band at 145 kD in the starting material, was also bound by all three SH3 domains. However, endophilin clearly showed the highest affinity for this polyphosphoinositide phosphatase. Syndapin I and especially Abp1 SH3 domains bound less well in our in vitro examinations (Fig. 1 c). All these interactions were SH3 domain specific, since neither GST alone nor a mutated SH3 domain (Qualmann et al., 1999) showed a coprecipitation of any of these proteins (Fig. 1 c). Also, the NH_2-terminal half of Abp1, comprising the ADF-H domain and the highly charged helical domain, did not bind to any of these proteins. The NH_2-terminal half of Abp1, however, was able to bind to actin filament fragments in the extracts (Fig. 1 c). This interaction could not be detected by blot overlay because Abp1 binds to F- but not G-actin (Kessels et al., 2000). To formally prove that the direct interaction of the Abp1-SH3 domain with a 100-kD band in Fig. 1, a and b, represents an interaction with dynamin, as detected in Fig. 1 c, we immunoprecipitated this GTPase with the antidynamin antibody Hudy1, separated the protein material by SDS-PAGE, blotted it to nitrocellulose, and overlayed the blot with the Abp1-SH3 domain. Precipitated dynamin, as detected by antidynamin antibodies different from the antibody Hudy1 used for immunoprecipitation, was indeed recognized by the Abp1-SH3 domain (Fig. 1 d).

Abp1 and F-actin Colocalize during Synaptogenesis and at Synapses of Mature Primary Hippocampal Neurons

Most of the binding partners of the Abp1 SH3 domain are brain-specific or brain-enriched proteins. This prompted us to analyze the Abp1 localization in the neuronal context. Primary hippocampal neurons at different stages of development were immunolabeled for Abp1. Abp1 displayed a relatively uniform localization in young primary neuronal cultures (2 and 6 d; data not shown). Abp1 was slightly enriched in growth cones, reminiscent of its accu-

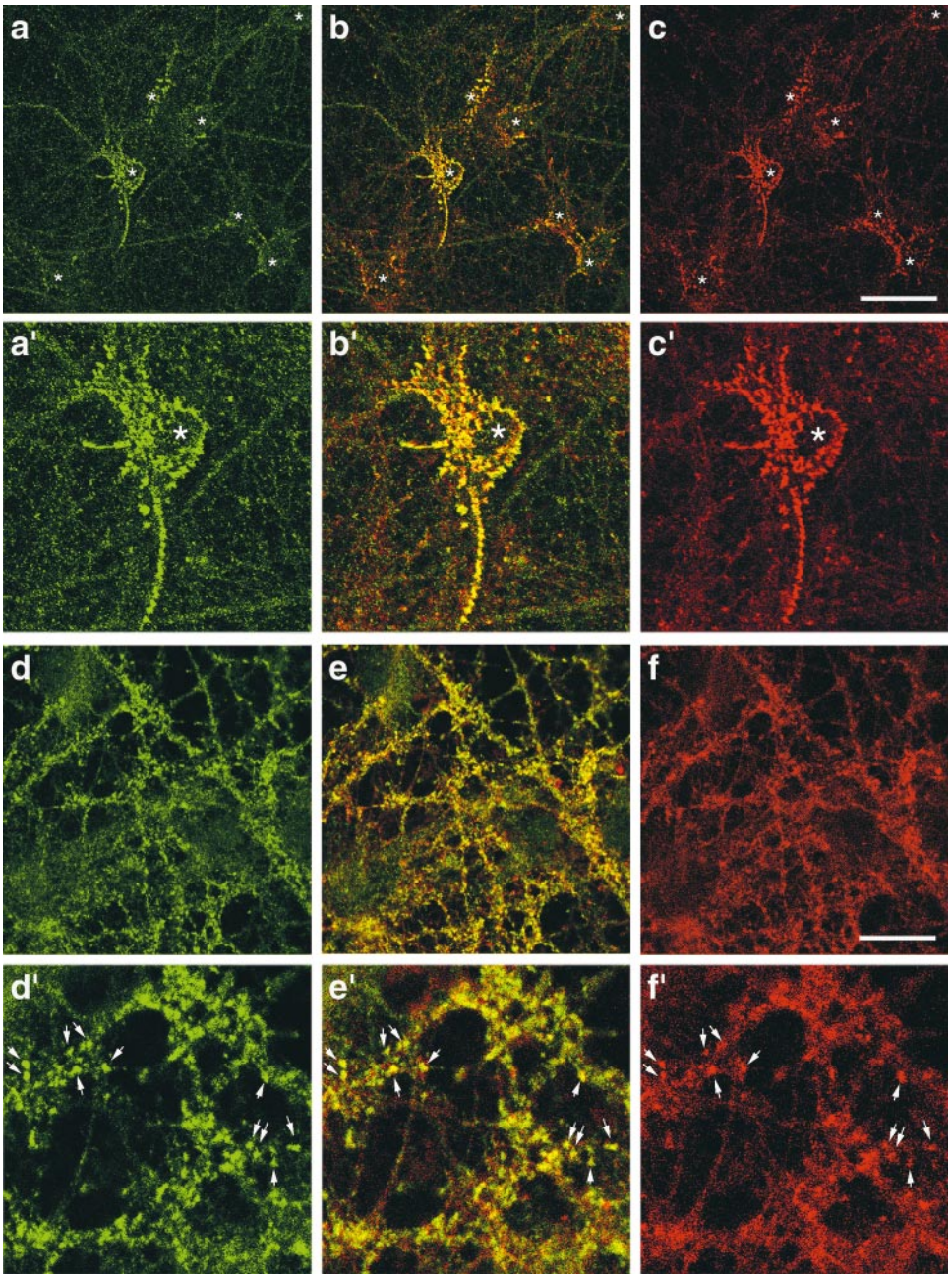

Figure 2. Colocalization of Abp1 and F-actin by confocal immunofluorescence microscopy. Primary hippocampal neurons kept in culture for 9 d displayed Abp1 accumulations in the extended peripheries of cell bodies as well as a cytosolic and neuritic immunostaining (a). F-actin was localized similarly (c), also seen in the merged image (b) and in the enlargements of the central areas of the images (a′–c′). (d–f) Neurons kept in culture for 20 d. At synapses, Abp1 (d) and F-actin (f) colocalize, as seen in the merged image (e) and in the enlargements of an area in the upper center of d–f (d′–f′). Stars in a–c and a′–c′ mark positions of cell bodies and arrows in d′–f′ mark selected examples of actin- and Abp1-rich postsynaptic structures. Bar: (c) 20 μm, (f) 10 μm.

mulation in lamellipodial areas in nonneuronal cells (data not shown; Kessels et al., 2000). This situation changed with the onset of synaptogenesis. Cells kept in culture for 9 d contained spatially well-defined areas of Abp1 accumulation at the extended periphery of the cell bodies. Costaining with Texas red-phalloidin revealed that the sites of Abp1 accumulation were actin-rich (Fig. 2). Actin was strongly restricted to sites proximal to the cell bodies. Abp1 also exhibited a readily detectable neuritic staining (Fig. 2, a–c). After synaptogenesis was complete and the synapses were functional, Abp1 and F-actin still colocalized in many cells, but now showed a broader distribution reflecting the extremely high number of synapses present in the culture (Fig. 2, d–f). In mature neurons, F-actin is enriched in dendritic spines and postsynaptic densities (Matus et al., 1982). At the light microscopic level, Abp1 seems to localize similarly to actin at both stages of neuronal development examined (9 and 20 d), as well seen in the enlarged images (Fig. 2, a′–c′ and d′–f′). In the cases where Abp1 showed a staining, which appeared synaptic, it seemed to be more restricted spatially to these sites compared with F-actin, which appeared a little more diffuse (Fig. 2, d′–f′).

Abp1 and Dynamin Colocalize at Actin-rich Sites during Synaptogenesis in Primary Hippocampal Neurons

It was next important to ask whether a spatial overlap of Abp1 and F-actin with dynamin could be detected. We therefore performed Abp1/dynamin colocalization studies using primary neuronal cells at different stages of differentiation. At all times points analyzed, Abp1 and dy-

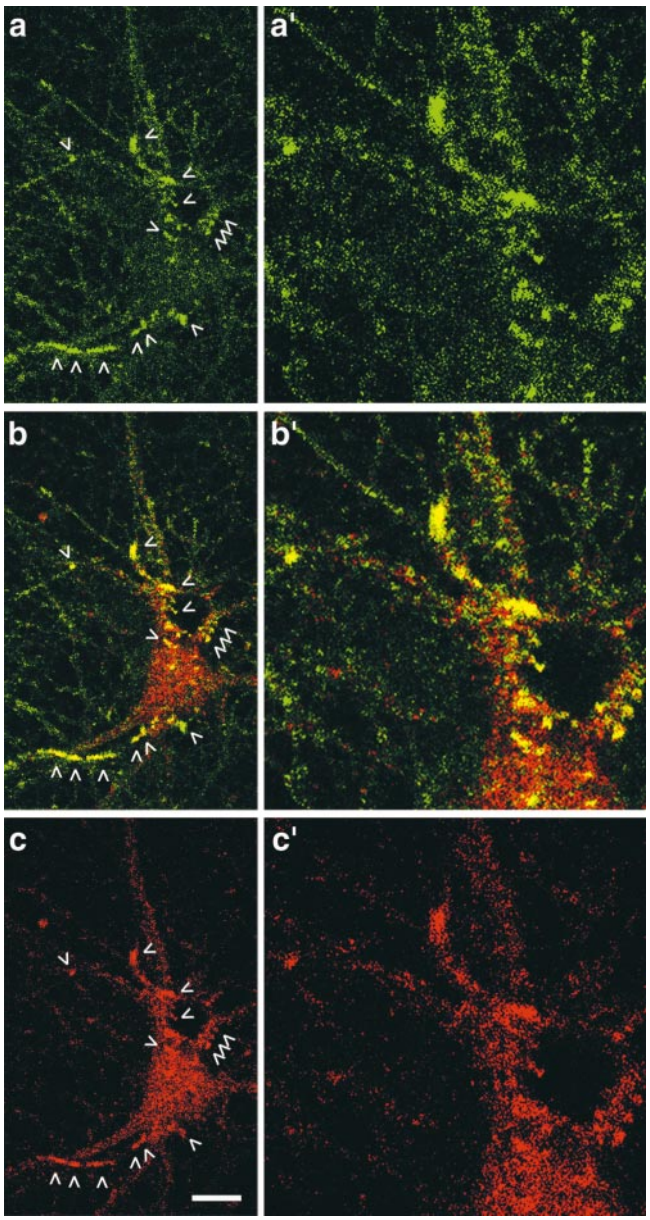

Figure 3. Colocalization of Abp1 (green) and dynamin (red) in primary hippocampal neurons by confocal microscopy. (a and a′) Abp1 strongly accumulated at defined sites in neurons kept in culture for 9 d (arrowheads). (c and c′) Besides cytosolic dynamin, sites of moderate dynamin accumulation proximal to the cell bodies were seen (arrowheads). These sites were immunopositive for Abp1, as seen in the merged images (b and b′). Note that subpools of both proteins did not spatially overlap (see neurites for Abp1 and cytoplasm for dynamin). a′–c′ are 2.5-fold enlargements of the center-right areas in a–c. Bar, 15 μm.

namin immunoreactivity showed some overlap at the light microscopical level (data not shown). Most prominently, in cells kept in culture for 9 d (Fig. 3), Abp1 showed strong accumulations near the cell body (Fig. 3, a and a′), similar to those seen in our Abp1/F-actin double labeling studies (Fig. 2). In these cells, dynamin was still cytosolic but also showed some enrichment at sites at the periphery of the cell bodies (Fig. 3, c and c′), where it colocalized with Abp1, as seen by the yellow color in the merged images (Fig. 3, b and b′). It should, however, be stressed that the

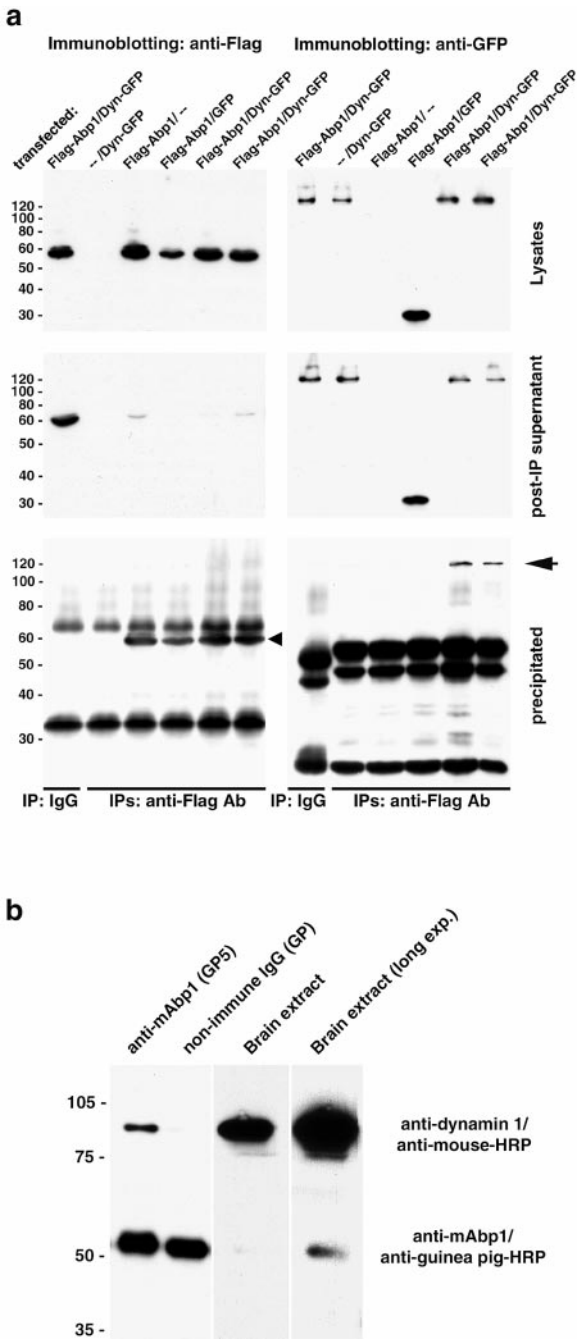

Figure 4. Coimmunoprecipitation of dynamin and Abp1. (a) Dynamin2aa-GFP coimmunoprecipitated (arrow) specifically with Flag-Abp1 from HEK cell extracts incubated with anti–Flag antibodies bound to protein G sepharose. Upper blots show material expressed by antitag immunostaining, middle blots show remaining protein in the post-IP supernatant, and bottom blots show immunoprecipitated Flag-Abp1 (left, arrowhead) and coimmunoprecipitated dynamin-GFP (right, arrow). Lysate and post-IP supernatant are 1/13 of the reaction. (b) Endogenous dynamin (detected by immunoblotting with the antidynamin antibodies) was specifically coimmunoprecipitated with Abp1 from rat brain extract with anti–Abp1 antibodies but not with equal amounts of unrelated guinea pig IgGs. Since Abp1 and IgGs both exhibit similar apparent molecular weights, the band of ~55 kD represents both IgG and Abp1 (left lane), solely IgG (second from left lane), and, in the next two lanes, only Abp1 signals are observed at 55 kD. One third of immunoprecipitated material was loaded. Starting material represents 20 μg of brain protein.

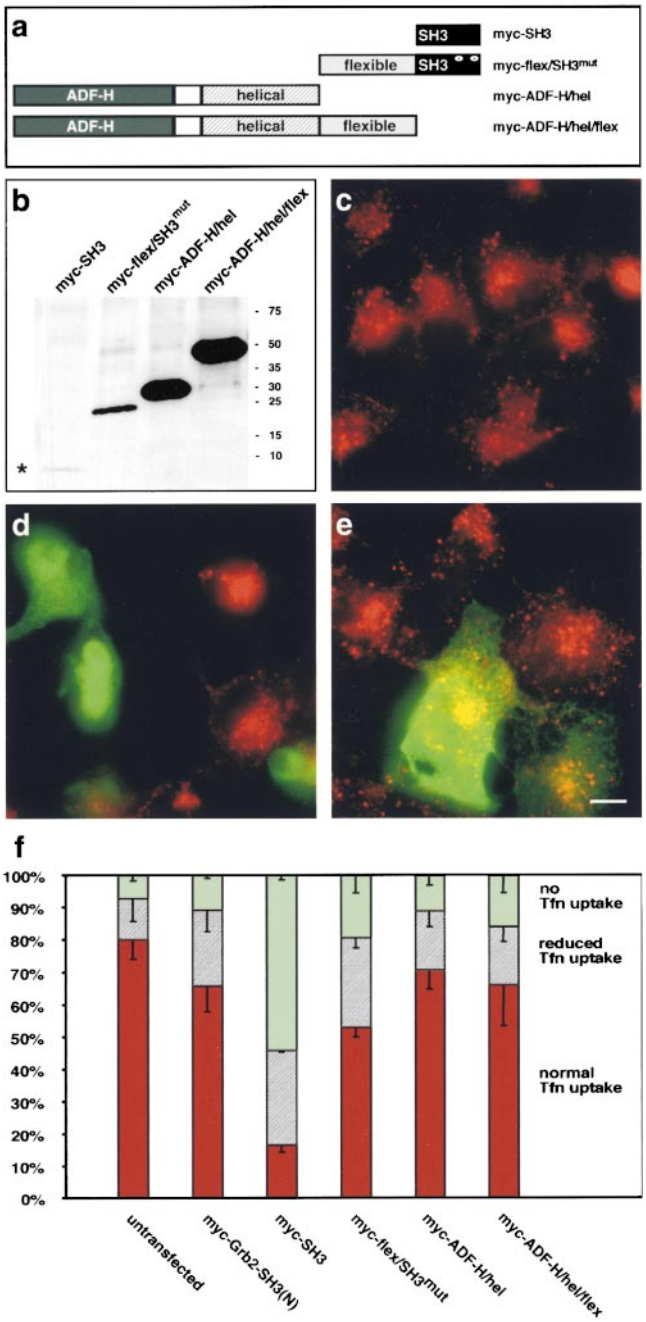

Figure 5. The Abp1 SH3 domain blocks endocytosis. (a) Schematic representation of myc-tagged Abp1 constructs used for transient transfections of Cos-7 cells. (b) SDS-PAGE and anti–myc immunoblotting of fusion proteins expressed in Cos-7 cells. The myc-SH3 construct (7 kD) is marked by a star. (c–e) Receptor-mediated endocytosis of Texas red-transferrin conjugates (red) in cells overexpressing Abp1 domains (green), merged images. (c) Untransfected cells. (d) Cells transfected with the Abp1-SH3 domain. (e) Cells overexpressing the actin-binding half of Abp1. Bar, 10 μm. (f) Quantitation of the results by assessing the percentages of cells lacking transferrin signal (block), displaying significantly reduced levels of uptake, and showing endocytosis capabilities similar to untransfected cells (data derived from group of cells showing high expression; data of lower expressing group of cells not shown, see text). Untransfected cells: 80.3 ± 6.0% normal, 12.7 ± 7.0 reduced, 7.3 ± 1.7% block, n = 359; myc-Grb2-SH3(N): 66.0 ± 8.0%, 23.5 ± 6.5%, 11.0 ± 1.0%, n = 359; myc-SH3: 16.5 ± 2%, 29.5 ± 0.5%, 54.5 ± 1.5%, n = 371; myc-flex/SH3^{mut}: 53.0 ± 2.9%, 27.7 ± 3.3%, 19.3 ± 5.6%, n = 701; myc-ADF-H/hel: 70.8 ± 5.8%, 18.3 ± 4.7%, 11.3 ± 3.3%, n = 614; myc-ADF-H/hel/flex: 65.9 ± 10.0%, 17.9 ± 4.4%, 16.3 ± 5.9%, n = 587.

spatial overlap of both proteins was restricted to these sites. Little dynamin was present in the extended neuritic network at this time point, and relatively low amounts of Abp1 were present in the cytoplasm, where dynamin was still readily detectable.

Thus, Abp1 appears to be associated with F-actin throughout the development of neurons and is most prominent at cortical sites at the time of synapse formation. During this stage, both actin and Abp1 colocalized with dynamin.

Abp1 Binds to Dynamin In Vivo

Our data obtained thus far suggested that Abp1 and dynamin interact physically. However, due to the fact that the two proteins did not quantitatively colocalize at the different stages of neuronal development studied, it was important to examine whether they actually interact in vivo. We therefore performed coimmunoprecipitation studies. On one hand, we used epitope-tagged proteins expressed in HEK cells. Flag-tagged Abp1 was immunoprecipitated almost quantitatively with anti–Flag antibodies (Fig. 4 a, arrowhead); i.e., very little protein remained in the post-IP supernatant. Unrelated IgG did not precipitate Flag-tagged Abp1. Further controls showed that the coprecipitation of dynamin is dependent on GFP-Abp1 expression and that this result is specific for Abp1, whereas GFP alone did not lead to any dynamin coprecipitation. Dynamin2aa-GFP coimmunoprecipitated specifically with the anti–Abp1 antibody/Abp1 immunoaggregate, but not with unrelated IgGs (Fig. 4 a, arrow). Approximately 50% of the total dynamin2aa-GFP was cleared from the post-IP supernatant by Abp1 immunoprecipitation (Fig. 4 a). Since the amount of dynamin in control incubations did not decline, this reduction is not due to proteolytic degradation during the incubation. The dynamin remaining in the post-IP supernatant may reflect (a) dynamin not bound to Abp1 but to other SH3 domain-containing proteins, (b) dynamin in a putative noninteractive state, and/or (c) dynamin expressed in cells, which do not coexpress Flag-Abp1 or express subequimolar levels of Flag-Abp1.

We also performed coimmunoprecipitation studies using adult rat brain extracts. The anti–Abp1 antibody GP5 coprecipitated dynamin, whereas the same amount of an unrelated guinea pig IgG did not; again, only a subpool of dynamin is precipitated along with Abp1 (Fig. 4 b). Both sets of experiments demonstrate that dynamin indeed associates with Abp1 in vivo.

Abp1 SH3 Domain Overexpression Blocks Receptor-mediated Endocytosis In Vivo

The association of Abp1 with the large GTPase dynamin via a proline-rich domain/SH3 domain interaction potentially creates a direct functional connection of the cortical actin cytoskeleton and the control of endocytic fission reactions by dynamin. Dynamin1 is an essential component in the formation of clathrin-coated vesicles in receptor-

mediated endocytosis (Damke et al., 1994). To address the in vivo relevance of the Abp1–dynamin interaction, we tried to interfere with dynamin function by transient overexpression of different domains of Abp1 (Fig. 5 a) in Cos-7 cells. These proteins were all myc-tagged to directly compare expression levels within individual cells. Additionally, expression of the myc-tagged fusion proteins was monitored by Western blotting (Fig. 5 b). The low amount of SH3 domain detected reflects both a relatively low transfection efficiency of this construct and the lower expression levels observed with this Abp1 domain (Fig. 5 b). We assayed the ability of these cells to endocytose fluorescently labeled transferrin. In untransfected cells, the Texas red-transferrin signal is readily detectable in the perinuclear region after 30 min of uptake (Fig. 5 c), and only a very minor fraction of cells does not take up transferrin (Fig. 5 f). Most of these cells are in mitosis. Cells transfected with the Abp1-SH3 domain, in contrast, showed inhibited endocytosis. In many cells, no Texas red-transferrin signals were detected (Fig. 5 d). Others showed significantly reduced levels of internalized transferrin. Neighboring untransfected cells displayed normal uptake. Quantification of the overexpression phenotype confirmed that the effect was dramatic (Fig. 5 f). 54.5 ± 1.5% of the transfected cells showed no uptake. Additionally, a large portion of transfected cells showed significantly reduced signals of endocytosed transferrin (29.5 ± 0.5%). Only a minor fraction of cells overexpressing the Abp1-SH3 domain displayed transferrin uptake levels similar to those of untransfected cells. This inhibitory effect of the Abp1 SH3 domain on receptor-mediated endocytosis was already detected in cells expressing only low amounts of the myc-tagged fusion protein (see also Fig. 5 b). Cells exhibiting only low expression levels of the recombinant proteins were scored and quantified separately (data not shown).

We compared these results with those for Cos-7 cells transfected with another SH3 domain, the NH_2-terminal SH3 domain of Grb2, which was reported to bind to dynamin in vitro (Gout et al., 1993). In contrast to the Abp1-SH3 domain, overexpression of the NH_2-terminal SH3 domain of Grb2 did not result in a strong block in endocytosis in vivo. Only a small fraction of cells showed some reduction in transferrin uptake (Fig. 5 f). These results are consistent with data reported by Wigge et al. (1997).

We next examined the effects of overexpression of the other Abp1 domains on receptor-mediated endocytosis. The flexible domain of Abp1 contains the two Src phosphorylation sites (Larbolette et al., 1999). The tyrosine kinase Src, which also phosphorylates the clathrin heavy chain, may play a role in receptor-mediated endocytosis (Wilde et al., 1999). Overexpression of the flexible domain alone, however, was precluded due to expression problems. We circumvented this problem by introducing two mutations into the Abp1-SH3 domain (P422L and G425R; numbers according to the long, codon 235-containing mouse Abp1 sequence) that are known to disrupt any SH3 domain/polyproline binding (Clark et al., 1992), and overexpressed a combination of flexible and inactivated SH3 domain (Fig. 5, a and b). The effects on endocytosis were modest. Only a minor fraction of the transfected cells showed a complete block of endocytosis, although almost half of the cells showed some defects (Fig. 5 f; block, 19.3 ± 5.6%; reduced, 27.7 ± 3.3%; normal, 53.0 ± 2.9%; $n = 701$). Since this minor perturbation of endocytosis was also observed by overexpression of the Abp1ΔSH3 construct (myc-ADF-H/hel/flex), we conclude that this effect is due to the flexible domain and does not represent a negative effect of the inactivated SH3 domain (Fig. 5 f).

Since Abp1 seems to represent a functional link between actin and endocytosis, it was important to determine the endocytosis capabilities of cells overexpressing the F-actin–binding part of Abp1. Overexpression of myc-ADF-H/hel had no significant negative effects on endocytosis, despite extremely high protein expression levels (Fig. 5, e and f).

The Block of Endocytosis Caused by Overexpression of the Abp1 SH3 Domain Can Be Suppressed by Dynamin Co-overexpression

We have shown that Abp1 interacts with dynamin in vitro and in vivo through its SH3 domain (Figs. 1 and 4). The overexpression phenotype of the SH3 domain implicates Abp1 protein interactions in endocytic functions (Fig. 5). To prove that the endocytosis impairment observed in Abp1-SH3 domain–overexpressing cells is indeed due to the Abp1/dynamin interaction, we cotransfected Cos-7 cells with an HA-dynamin1 plasmid together with constructs encoding for the Abp1-SH3 domain and for the entire COOH-terminal half of Abp1 (myc-flex/SH3). Quantifications of transferrin uptake-positive cells demonstrated that endocytic function was restored upon cooverexpression of wild-type dynamin (Fig. 6). Cells overexpressing dynamin and the COOH-terminal half of Abp1 took up transferrin with a rate similar to cells overexpressing the mutated COOH-terminal half of Abp1; i.e., a protein with an inactivated SH3 domain (rescue 81.0 ± 3.7%). The remaining slight inhibitory effect of both of the latter constructs represents the effect of the overexpression of the flexible, Src kinase target domain (Fig. 6 a). The influence of this domain on endocytosis was thus independent of dynamin function. When both the extend of double transfection (quantified by double immunofluorescence staining; data not shown) and the not rescuable effect of the flexible domain were considered (theoretically achievable rescue) the rescue was 104.7 ± 8.7%.

Cells cooverexpressing the SH3 domain of Abp1 together with dynamin were rescued completely (rescue 96.5 ± 3.8%). The quantification data obtained from these cells are indistinguishable from those of wild-type cells or cells overexpressing dynamin alone (Fig. 6 b). Dynamin was thus able to overcome the endocytosis block induced by the Abp1 SH3 domain in almost all cotransfected cells.

Association of Abp1 with Dynamin-containing Sites upon Growth Factor Stimulations of NIH3T3 Fibroblasts

Our data indicate that Abp1 may, via its actin-binding modules and its SH3 domain, link actin and endocytosis. However, Abp1 does not appear to colocalize with endosomal compartments (i.e., with late states of endocytosis) (Kessels et al., 2000), nor does it seem to be a stable component of the endocytic coat because it was not found to be enriched on clathrin-coated vesicles (Engqvist-Goldstein et al., 1999). In resting cells, Abp1 is not associated

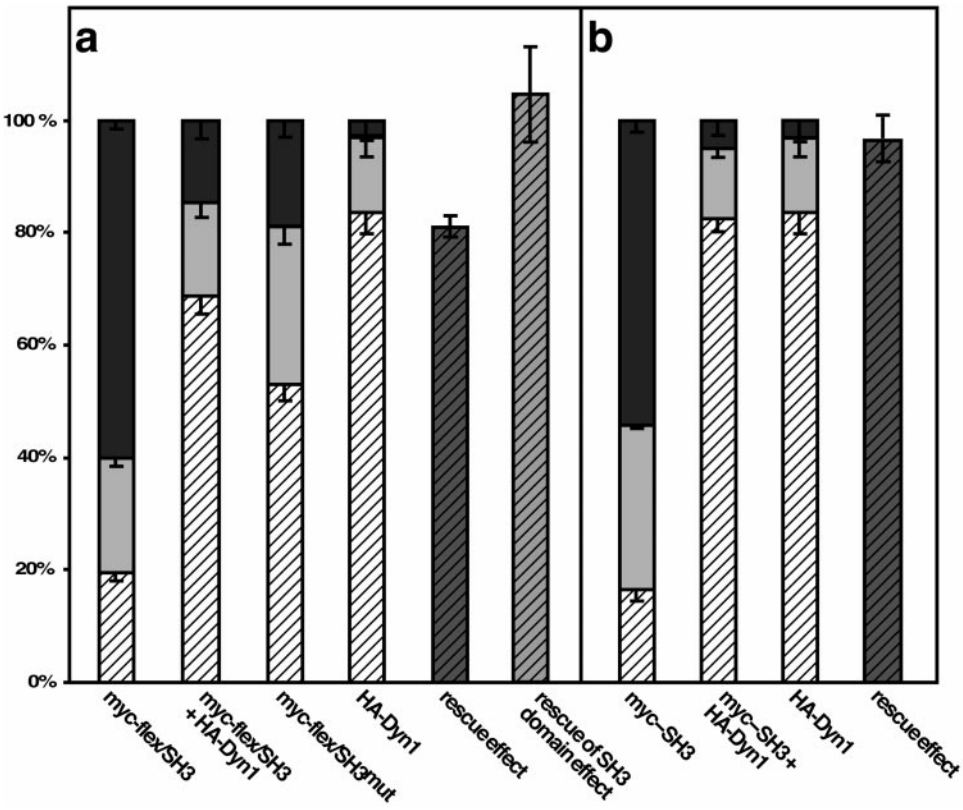

Figure 6. Cooverexpression of dynamin rescues the endocytosis block caused by overexpression of the Abp1 SH3 domain. Cos-7 cells were double transfected with HA-dynamin1 and myc-Abp1 constructs. Quantification of transferrin uptake, as in Figs. 5 and 9, dark grey, no transferrin uptake, light grey, significantly reduced levels of uptake, and hatched cells show a transferrin uptake comparable with wild-type cells. Myc-(Abp1-)Flex/SH3–overexpressing cells were rescued up to a level similar to that caused by the flexible domain alone (a). Myc-(Abp1-)SH3–overexpressing cells were rescued up to a level similar to wild-type or HA-dynamin–overexpressing cells (b). Myc-flex/SH3: 19.5 ± 1.5% normal, 20.5 ± 1.5% reduced, 60.0 ± 3.0% block, n = 447; myc-flex/SH3 + HA-dynamin1: 68.7 ± 3.2%, 16.5 ± 2.5%, 14.75 ± 0.75%, n = 237; myc-flex/SH3^{mut}: 53.0 ± 2.9%, 27.7 ± 3.3%, 19.3 ± 5.6%, n = 701; HA-dynamin1: 83.5 ± 3.7%, 13.7 ± 3.6%, 2.85 ± 0.05%, n = 213; hatched dark grey column: rescue effect, 81.0 ± 3.75 % (cotransfection rate of 96.5% was taken into consideration). This value represents 104.7 ± 8.7% of theoretically achievable maximal rescue (the fact that effect of SH3 domain but not that of the flexible domain can be rescued was taken into consideration; hatched light grey column). Myc-SH3: 16.5 ± 2%, 29.5 ± 0.5%, 54.5 ± 1.5%, n = 371; myc-SH3 + HA-dynamin1: 82.6 ± 2.3%, 12.7 ± 1.8%, 4.65 ± 0.45%; HA-dynamin1: 83.5 ± 3.7%, 13.7 ± 3.6%, 2.85 ± 0.05%, n = 213; hatched dark grey column: rescue effect (in case of myc-SH3 overexpression, identical to the achievable maximal rescue of SH3 domain effect), 96.5 ± 3.8% (cotransfection rate of 92.0% was taken into consideration).

with the actin cytoskeleton either, but we have discovered that the association of Abp1 with cortical actin structures is controlled by signaling pathways converging on this protein (Kessels et al., 2000). We therefore used conditions that caused a redistribution of Abp1 to sites of high actin dynamics (i.e., the leading edge of growth factor-treated NIH3T3 fibroblasts) to examine its participation in the endocytic process. We asked whether sites of endocytosis would contain Abp1 in stimulated cells. Short perforations of these growth factor–treated cells resulted in a retainment of Abp1 at the periphery of lamellipodia and at some puncta scattered throughout the cell cortex (Kessels et al., 2000). We arrested endocytosis by incubation at low temperature. Under these conditions, we were able to demonstrate that at the cortex of NIH3T3 cells, dynamin-containing sites labeled by the antibody Hudy1 were almost always also immunopositive for Abp1 detected by the antibody GP5 (Fig. 7). Coimmunolabelings with oppositely labeled secondary antibodies led to similar results (data not shown). The accumulation of Abp1 at the leading edge of lamellipodia was preserved under the conditions applied (Fig. 7, a and d). The Abp1-rich leading edge was, however, virtually free of any dynamin staining using the monoclonal antibody Hudy1. Thus, either dynamin seems not to be recruited to the leading edge by the subcellular shift of the majority of Abp1, or it is not detectable with Hudy1 at this location. In serum-starved cells, no colocalization was detected (Fig. 7, g–i). Under these conditions, most of the Abp1 is readily extracted and little signal remains. Also in resting cells, only little overlap of Abp1 and dynamin immunolocalization was observed after permeabilization (data not shown). Thus, Abp1's detection at dynamin-rich sites seems to depend on growth factor receptor activation.

Dynamin-rich Sites at the Cortex of NIH3T3 Cells Stimulated with Growth Factors Contain Endocytic Coat Components

Several observations have suggested that dynamins may play an as yet unidentified cytoskeletal role in addition to their endocytic function (for review, see McNiven et al., 2000). At least dynamin2aa was observed at actin-rich sites within cells, which seem independent of sites of endocytosis (Cao et al., 1998; Ochoa et al., 2000). It was thus important to examine whether the dynamin-rich sites detected by the antibody Hudy1, which were observed to be Abp1 immunopositive under conditions also leading to a recruitment of Abp1 to actin-rich lamellipodia, were sites of endocytosis, or whether they reflect a putative cytoskeletal role of dynamin. We therefore stained cells, which had been stimulated and permeabilized as before, with the monoclonal Hudy1 antibody (Fig. 8 a) and a poly-

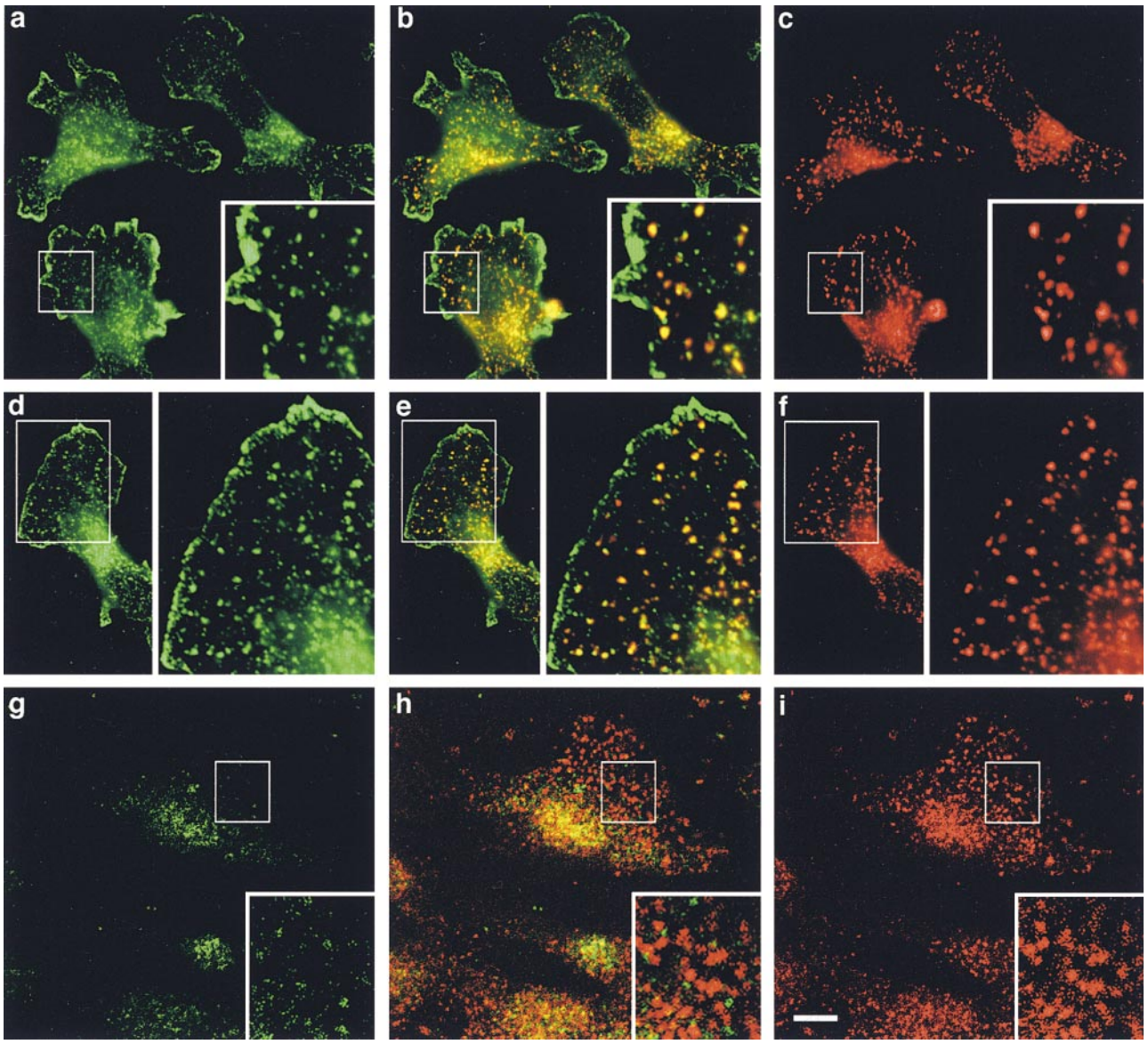

Figure 7. Association of Abp1 with dynamin-containing pits upon growth factor stimulations of 3T3 fibroblasts. NIH3T3 fibroblasts were replated onto fibronectin-coated coverslips, stimulated with 300 ng/ml PMA and 5 ng/ml PDGF for 10 min, perforated with 0.02% saponin and subsequently fixed and processed for immunofluorescence microscopy (a–f). The lamellipodial accumulation of Abp1 (Kessels et al., 2000) was observable under these conditions (a and d). In addition, a widely distributed, punctate Abp1 immunostaining was detected (a and d). (c and f) Immunostaining of dynamin using the monoclonal antibody Hudy1 at perinuclear and cortical sites. (b and e) Merged images show that dynamin-containing sites are in almost all cases also immunopositive for Abp1 as especially well seen in extended lamellipodial areas (d–f). In contrast, in serum-starved cells, Abp1 (g) is readily extracted and the remaining protein shows no colocalization with dynamin (g–i). Inserts are enlargements of the marked areas. Bar, 10 μm.

clonal antibody against the clathrin coat component Hip1R (Engqvist-Goldstein et al., 1999) (Fig. 8 c). Besides some labeling in and/or near the nucleus, which seemed to be a result of our membrane perforations, both antibodies detected their antigen in cortical spots resistant to the perforation procedure (Fig. 8, a and c). Colocalization experiments demonstrated that the dynamin-rich sites detected by the monoclonal antibody Hudy1 were also positive for Hip1R (Fig. 8 b). We have previously also shown that Hip1R puncta at the cell cortex colocalize quantitatively with the adaptor protein AP2 detected with the monoclonal antibody AP6 (Engqvist-Goldstein et al., 1999). The perforation-resistant, dynamin-rich areas at the cell cortex also contain eps15 (Fig. 8, d–f), another component of clathrin coats (Tebar et al., 1996). Eps15 immunostaining is strongest at puncta at the periphery and decreases towards the center of the cells (Fig. 8 f), whereas dynamin labeling shows the opposite gradient (Fig. 8 d). However Eps15 and dynamin show clear colocalization (Fig. 8 e).

Additionally, we performed a double staining of Abp1 with another coat component, the adaptor protein complex AP2. Similar to the results obtained with the antidynamin antibody, puncta labeled by anti–AP2 antibodies

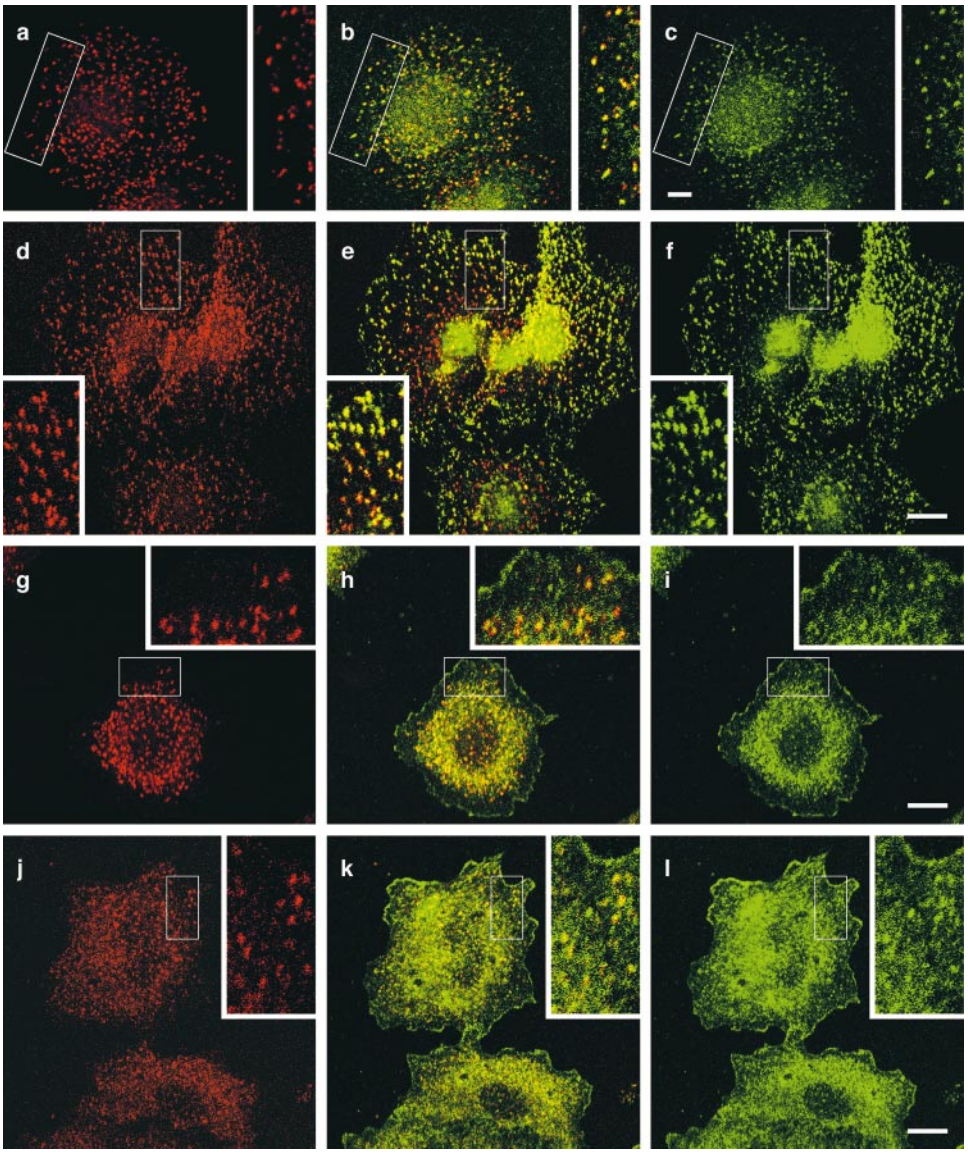

Figure 8. Cortical dynamin-rich sites in NIH3T3 cells, which become Abp1 immunopositive after receptor activation, are sites of endocytosis. Dynamin (a) and the endocytic coat component Hip1R (c) colocalize (b, merge) in cells stimulated with growth factors, as observed by confocal microscopy. Colocalization of dynamin (d) and eps15 (f), as seen in the merged image (e). Colocalization of AP2 (g) and Abp1 (i) at puncta at the cell cortex, but not at the leading edge of the cell; as seen in the merged image (h). (j–l) In nonperforated activated cells, the cytosolic pool of Abp1 largely obscures the weak Abp1 immunostaining (l) at sites of endocytosis [here marked by anti–AP2 immunostaining (j)]. Inserts represent enlargements of the areas boxed in a–l. Bars, 10 μm.

were also immunopositive for Abp1. Thus, the punctate sites at the cell cortex, which became Abp1-positive upon stimulation with growth factors, seem to represent sites of endocytosis (Fig. 8, g–i).

To exclude that the observed association of Abp1 with sites of endocytosis is due to a postperforation movement of the protein, colocalization studies were performed in nonperforated cells. In these cells, a colocalization of AP2 and Abp1 is partially obscured by the extractable cytoplasmic pool of Abp1 (Fig. 8, j–l); however, in flat and extended areas of the cells, it is often possible to see that AP2 puncta are indeed positive for Abp1 (Fig. 8, j–l, insets).

Therefore, Abp1 is indeed observed at dynamin-rich sites, which contain endocytic machinery and therefore most likely represent sites of endocytosis. These results are consistent with the observation by Ochoa et al. (2000) that dynamin-rich sites stained by the antibody Hudy1 generally contain endocytic machinery, whereas dynamin localized to actin-rich structures was not observable using this antibody.

Endocytosis Is Restored by Readdition of the Two Actin-binding Modules of Abp1 to the Overexpression Constructs

The localization of Abp1 at dynamin-rich sites of endocytosis upon growth-factor stimulation suggested that Abp1 could support receptor-mediated endocytosis by a mechanism regulated by the same signals as its involvement in actin dynamics at the actin-rich leading edge. We therefore decided to directly address the possibility that Abp1's actin-binding modules might participate in the endocytic function of this protein and systematically added back domains to the SH3 domain overexpression construct (Fig. 9 a). We then assayed receptor-mediated endocytosis in cells overexpressing these constructs (Fig. 9 b).

As shown in Fig. 5, overexpression of the SH3 domain (myc-SH3) strongly inhibited endocytosis (Fig. 9 b). Readdition of the flexible domain to the SH3 domain (myc-flex/SH3) did not result in any beneficial changes. In fact, even more cells showed a complete lack of transferrin uptake (Fig. 9 b). We next added back the helical domain; i.e., one of the actin-binding domains. Overexpression of such a con-

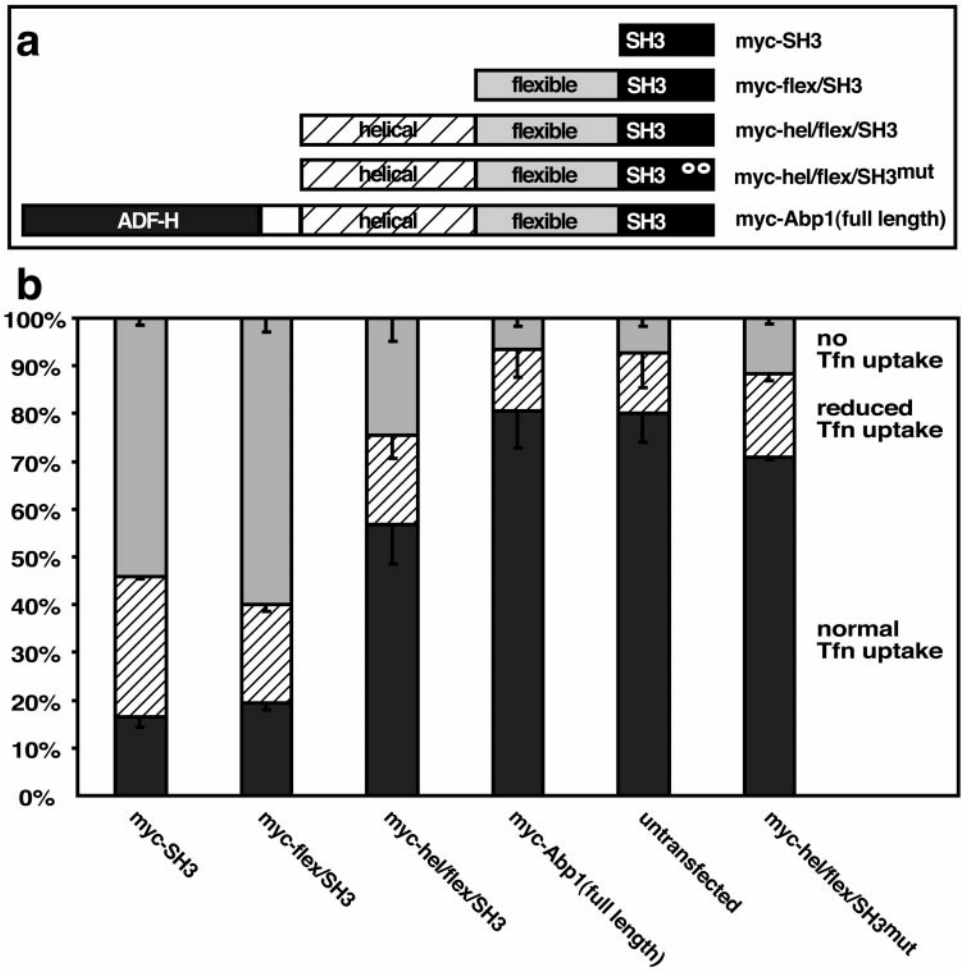

Figure 9. Sequential readdition of Abp1's actin-binding modules to the SH3 domain overexpression construct leads to a restoration of endocytosis in transfected Cos-7 cells. (a) Scheme of the overexpression constructs used. (b) Quantitation, myc-SH3: 16.5 ± 2% normal, 29.5 ± 0.5% reduced, 54.5 ± 1.5% block, n = 371; myc-flex/SH3: 19.5 ± 1.5%, 20.5 ± 1.5, 60.0 ± 1.5%, n = 447; myc-hel/flex/SH3: 56.7 ± 8.3%, 18.7 ± 4.9%, 24.3 ± 4.9%, n = 429; myc-Abp1(full length): 81 ± 7.8%, 13.0 ± 5.7%, 6.7 ± 1.7%, n = 448; untransfected cells: 80.3 ± 6.0%, 12.7 ± 7.0, 7.3 ± 1.7%, n = 359; myc-hel/flex/SH3^{mut}: 70.3 ± 0.5%, 17.3 ± 1.3%, 11.7 ± 1.3%, n = 410.

struct (myc-hel/flex/SH3) caused a much reduced endocytosis perturbation. About half of the cells expressing myc-hel/flex/SH3, a construct that still does contain the endocytosis-blocking SH3 domain, now endocytosed transferrin as wild-type cells did (Fig. 9 b). This improvement was not due to lower expression levels, since the expression levels observed for myc-hel/flex/SH3 were similar to those of the endocytosis-inhibiting myc-flex/SH3 construct both in extracts and in individual transfected cells (data not shown).

The difference between overexpression of the myc-hel/flex/SH3 construct compared with overexpression of the COOH-terminal half could theoretically reflect a perturbation caused by overexpression of the newly added helical domain, while the SH3 domain is already correctly used in conjunction with this additionally added actin-binding module. As a control, we designed a similar construct with a mutated SH3 domain. Overexpression of this construct should reveal any potential disadvantageous effects of overexpressing a combination of helical and flexible domain. However, consistent with our observation that a combination of ADF-H and helical domain did not perturb endocytosis, no negative effects of an excess of the helical domain on endocytosis were observed (Fig. 9 b). We thus conclude that we indeed observed a partial restoration upon overexpression of the construct lacking the ADF-H domain and not a secondary inhibitory overexpression effect of the helical domain on top of a SH3 domain-dependent Abp1 function fully restored by combining the SH3 domain with one actin-binding module.

Finally, we asked whether the ADF-H domain, the second F-actin–binding domain of Abp1, and the helical domain could act synergistically. When the NH_2-terminal ADF-H domain was also added back to the expression construct, the SH3 domain overexpression phenotype was completely suppressed and endocytosis was restored to wild-type levels (Fig. 9 b), even though expression levels of this full-length construct, which again does contain the endocytosis-blocking SH3 domain, were ~5–10× higher than those of the endocytosis-blocking myc-flex/SH3 construct (data not shown). This result suggests that in addition to Abp1's SH3 domain, both actin-binding domains might be involved in Abp1's role in dynamin-controlled receptor-mediated endocytosis. Abp1 thus appears to represent both a functional and a physical link between the cortical actin cytoskeleton and the endocytic machinery.

Discussion

The actin cytoskeleton has been implicated in endocytosis in mammalian cells, yet few molecular links have been identified (reviewed in Qualmann et al., 2000). Abp1 is the first F-actin–binding protein for which a functional role at the interface of actin and endocytosis is suggested from in vivo data. Abp1 is an Src kinase target that we have shown

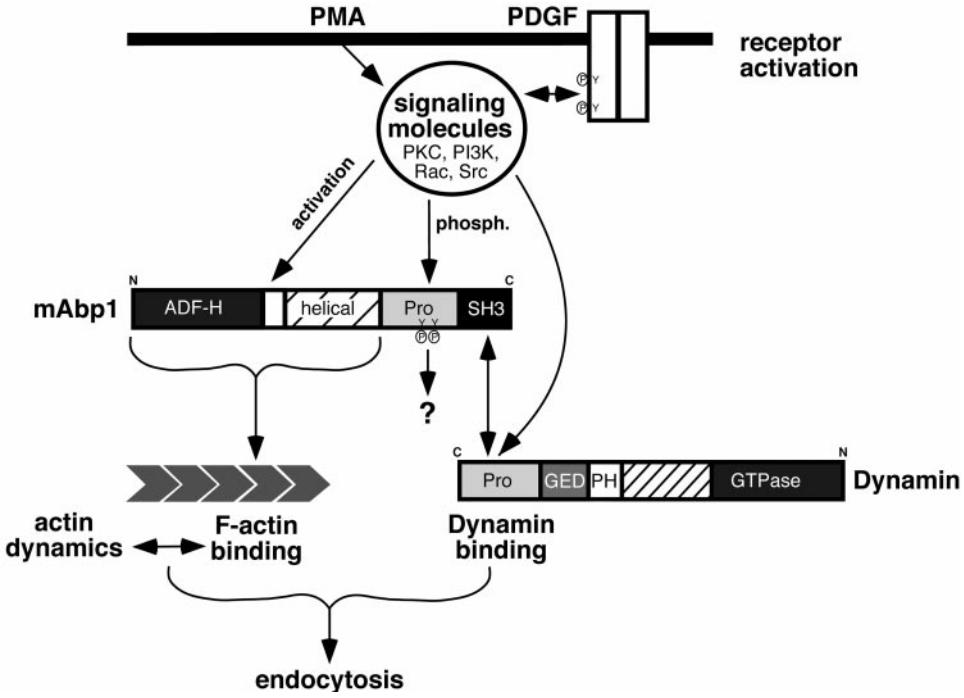

Figure 10. Schematic representation of Abp1 function at the interface of endocytosis and actin cytoskeleton.

to bind to the GTPase dynamin. Abp1 may therefore associate with the endocytic machinery, which is assembled and activated in response to outer stimuli. This possibility is consistent with data from yeast. Yeast Abp1 is a component of the dynamic cortical actin cytoskeleton and can interfere with cell polarity and polar organization of the actin cytoskeleton upon overexpression (Drubin et al., 1988). It has been implicated in cAMP signaling and endocytosis by its protein interactions (Lila and Drubin, 1997) and by genetic analysis (Wesp et al., 1997).

Here we have shown that the SH3 domain of mammalian Abp1 interacts with dynamin in vitro and in vivo. Overexpression of the Abp1 SH3 domain blocks endocytosis in Cos-7 cells (Fig. 5). Overexpression of other SH3 domains that bind to dynamin (i.e., those of amphiphysins and syndapins) led to similar inhibition of receptor-mediated endocytosis (Wigge et al., 1997; Qualmann and Kelly, 2000). We were able to demonstrate that the impairment of endocytosis caused by the SH3 domain of Abp1 is dependent on interaction with dynamin, while the more moderate effect of the flexible Src kinase target domain is not. The fact that the SH3 domain overexpression phenotype was completely suppressed by dynamin cooverexpression strongly implicates Abp1 in dynamin functions. Our analyses furthermore suggest that Abp1 may serve both as a functional and physical link between receptor-mediated endocytosis and the actin cytoskeleton and that, besides Abp1's dynamin-binding SH3 domain, both of Abp1's actin-binding modules seem to be involved in this function (Fig. 10).

One could argue that while the isolated SH3 domain of Abp1 binds to dynamin, and thus interferes with endocytosis, full-length Abp1 is not involved in endocytosis. Several results argue against this. First, endogenous Abp1 was coimmunoprecipitated with dynamin from rat brain extracts. Thus, mammalian Abp1 associates with dynamin in vivo. Second, such an interaction was supported by the observed colocalization of both proteins at actin-rich sites in neurons. Third, also a recombinant Flag-tagged fusion protein of Abp1 was demonstrated to bind to dynamin in vivo. Fourth, endogenous Abp1 was recruited to dynamin-rich sites of receptor-mediated endocytosis in NIH3T3 cells, specifically when receptors were activated. Therefore, it is likely that Abp1 participates in endocytic processes.

Besides their crucial function in endocytosis, GTPases of the dynamin family may play a yet unidentified cytoskeletal role (for review, see McNiven et al., 2000). Thus far, the hints have been indirect. However, Cao et al. (1998) reported that green fluorescent protein fusion proteins of dynamin2 splice variants localize to lamellipodia. In addition, as Ochoa et al. (2000) demonstrated, dynamin2aa localized to podosomes, F-actin–rich structures that surround tubular plasma membrane invaginations in cells expressing activated Src. The study also showed that a putative cytoskeletal function of dynamin can be separated from its role in endocytosis and that podosomes lack endocytic coat components. Also, podosomal areas of the cells were negative for transferrin uptake. However, it is unlikely that the Abp1/dynamin interaction we discovered solely reflects this putative cytoskeletal function of dynamin. First, we found that upon growth factor treatments of NIH3T3 cells, Abp1 relocalized to both actin-rich lamellipodia and to dynamin-rich sites at the plasma membrane, while lamellipodia were free of anti-dynamin staining. Second, we examined the dynamin-rich sites detected by the monoclonal antibody Hudy1 more closely, and found them to contain eps15 and Hip1R, both components of clathrin coats (Tebar et al., 1996; Engqvist-Goldstein et al., 1999). Therefore, these dynamin-rich sites clearly represent sites of endocytosis. This is consistent with the observed Abp1/AP2 colocalization. Our results thus rather suggest that Abp1 participates in the organization of dynamic actin structures, and that this function, which is controlled by different signaling transduction pathways, also supports receptor-mediated endocytosis controlled by dynamin at punctate sites at the cell cortex (Fig. 10).

Strikingly, the relocalization of Abp1 to dynamin-rich sites, and the recruitment of Abp1 to the dynamic, actin-rich leading edge, are both responsive to growth-factor receptor activation. Currently, we do not know whether Abp1 is recruited to pre-existing dynamin-rich sites of endocytosis or whether a putative activation of Abp1 leads to the de novo establishment of such sites. Receptor activation is a positive stimulus for receptor endocytosis, and dynamin can be coimmunoprecipitated with growth factor receptors after their activation (Scaife et al., 1994). Recently, Src kinase–mediated tyrosine phosphorylation of dynamin has been shown to be required for clathrin-mediated G protein–coupled receptor endocytosis (Ahn et al., 1999). Src activation by EGF also led to a phosphorylation of clathrin heavy chains and may be involved in the recruitment of clathrin to the periphery. In Src kinase–deficient cells, clathrin remained at the TGN. Consistently, EGF uptake was slightly delayed in these cells (Wilde et al., 1999), while in Src kinase overexpressing cells the rate of EGF receptor endocytosis increased (Ware et al., 1997). In line with this, our results show that overexpressing the flexible Src target domain of Abp1 (i.e., a putative competition with endogenous kinase targets) also perturbs endocytosis and that this perturbation is independent of dynamin function because it cannot be rescued by dynamin cooverexpression.

Several roles for the actin cytoskeleton and for Abp1 in endocytosis would be plausible. They are not mutually exclusive. First, cortical F-actin could organize and constrain the endocytic machinery and Abp1 could serve as a signal-responsive cytoskeletal anchor for proteins binding to its SH3 domain; i.e., act as adaptor protein linking signals from membrane receptors to the actin cytoskeleton and to dynamin as part of the endocytic machinery. A spatially defined organization of endocytic sites has been described at the *Drosophila* neuromuscular junction (Roos and Kelly, 1999). Defined sites of clathrin-coated pit formation were also observed by Gaidarov et al. (1999). Since the lateral mobility of clathrin-coated pits increased upon treatments with the actin-sequestering drug latrunculin B, an association with the cortical actin cytoskeleton has been suggested (Gaidarov et al., 1999). This implicates an interaction with some cytoskeletal adaptor protein. Besides Abp1, Hip1R is also a very attractive candidate to serve this function. We identified the F-actin–binding protein Hip1R (Engqvist-Goldstein et al., 1999) as a mammalian homologue of the yeast protein Sla2. In yeast, deletions of the genes *SLA2* and *ABP1* are synthetic lethal (Holtzman et al., 1993). When the central coiled-coil region of Sla2 was deleted, a mutation of the *SLA2* gene that alone had no negative effects on endocytosis, endocytic uptake processes became dependent on the SH3 domain of Abp1 (Wesp et al., 1997). We demonstrated that Hip1R can be copurified with coat components such as clathrin and AP2, and that in vivo the central coiled coil domain was required for Hip1R's correct localization to clathrin-coated pits, whereas its COOH terminus binds to actin (Engqvist-Goldstein et al., 1999). Here, we also show that Abp1 may play a role in endocytosis. Thus, the synthetic lethality of *SLA2* and *ABP1* in yeast may reflect a functional redundancy of these two genes in connecting the cortical actin cytoskeleton to the endocytosis machinery.

As a second model for a role at the interface of actin and endocytosis, Abp1 may be recruited to sites of endocytosis via its binding to dynamin or may be involved in the de novo establishment of such sites. In neuronal cells, dynamin may form ring-like structures at the neck of invaginated clathrin-coated pits during the fission reaction (Takei et al., 1995). Localization of Abp1 to dynamin-rich sites of endocytosis could result in the recruitment of dynamic F-actin. The formation of such dynamic actin structures at the neck of constricted coated pits could create forces that might support dynamin-controlled fission, vesicle detachment, and/or vesicle movement away from the plasma membrane similar to the mechanism used to propel pathogens such as *Listeria monocytogenes* through a host cell. Since Abp1 colocalizes with the Arp2/3 complex and with dynamic F-actin structures at the leading edge of mammalian cells (Kessels et al., 2000; this study), and since it activates the Arp2/3 complex in yeast (Goode et al., 2000), it may play a role in formation of actin tails in association with endocytic membranes. In support of this possibility, we have recently observed that Abp1 is recruited to and is enriched in *Listeria* tails (Kessels, M.M., unpublished observations). Actin tails associated with endosomes, pinosomes, clathrin-coated vesicles, and secretory vesicles in vivo have been described in recent studies (Frischknecht et al., 1999; Merrifield et al., 1999; Rozelle et al., 2000), as have endosomes and lysosomes in in vitro systems (Taunton et al., 2000). The study by Rozelle et al. (2000) also showed that such actin tail structures are inducible by growth factors and phosphoinositides and seem to depend on signaling events involving tyrosine phosphorylations. We have previously shown that Abp1's actin-binding function was responsive to PDGF receptor signaling, but also to other signal transduction pathways, such as protein kinase C stimulation via phorbolesters or overexpression of a dominant-active Rac (Kessels et al., 2000). Abp1 also serves as an Src kinase target (Lock et al., 1998; Larbolette et al., 1999). Thus, several signal transduction pathways may converge on Abp1 and control its putative role in the formation of tails (Fig. 10).

The proposed function of actin and Abp1 in endocytosis may not be important in all cells or cellular compartments, a hypothesis supported by our characterization of Abp1 in the neuronal context. We did not see a quantitative overlap of Abp1 and dynamin at all stages of development. Both proteins colocalized at actin-rich sites at the onset of synaptogenesis, but colocalizations were less evident in cells at other developmental stages. As in growth factor–treated NIH3T3 cells, where the major pool of Abp1 was recruited to the leading edge, much of the cellular Abp1 localized to dynamic actin-rich structures; i.e., to spines and postsynaptic densities. However, compensatory endocytosis is a major dynamin1-controlled process in neurons and takes place in the presynapse. Currently, we do not know whether Abp1 is involved in dynamin function at the presynaptic side. However, dynamin has recently also been implicated in important postsynaptic endocytic processes. Similar to the involvement of dynamin in the agonist-dependent internalization of cell surface receptors leading to desensitization (Ahn et al., 1999), dynamin has recently been implicated in long-term depression (Napolitano et al., 1999). Consistent with this, Man et al. (2000) reported a role for

dynamin in postsynaptic AMPA receptor recycling. The fact that Abp1 was coimmunoprecipitated with only a subpool of dynamin in brain extracts may reflect Abp1's predominant association with such a postsynaptic dynamin pool. Long-term depression is a prominent form of synaptic plasticity and a basis for learning and memory. Our data suggest that in neurons, Abp1 may be of special importance during the onset of synaptogenesis and during postsynaptic processes that involve remodeling of the plasma membrane and of the cortical actin cytoskeleton. Our understanding of the mechanisms by which the actin cytoskeleton and endocytosis are functionally connected in different systems will increase with further studies of the interactions and functions of molecules at this interface, such as Abp1.

We thank Sandra L. Schmid for antibodies and for the HA-dynamin1 construct, Peter S. McPherson for antibodies, Mark McNiven for the dynamin2aa-GFP construct, and Brian Kay for the GST-Grb2-N-SH3 construct. We are grateful to Eckart D. Gundelfinger and Regis B. Kelly for their support and to Kathrin Hartung for her technical assistance. We also thank Narla Mohandes for generous support of this project and Christina Spilker for help with preparation of the primary hippocampal neurons.

This work was supported by an Otto-Hahn Research Award of the Max Planck Society and a fellowship from the Deutsche Forschungsgemeinschaft (Ke 685/1-1) as well as a grant of the Fond der Chemischen Industrie (661069) to M.M. Kessels, by National Institutes of Health grants GM-50399 and DK-32094 to D.G. Drubin, and by an Otto-Hahn Research Award of the Max Planck Society and a grant from the Deutsche Forschungsgemeinschaft (Qu 116/2-1) to B. Qualmann.

Submitted: 21 September 2000
Revised: 20 February 2001
Accepted: 22 February 2001

References

Ahn, S., S. Maudsley, L.M. Luttrell, R.J. Lefkowitz, and Y. Daaka. 1999. Src-mediated tyrosine phosphorylation of dynamin is required for beta2-adrenergic receptor internalization and mitogen-activated protein kinase signaling. *J. Biol. Chem*. 274:1185–1188.

Brodin, L., P. Löw, and O. Shupliakov. 2000. Sequential steps in clathrin-mediated synaptic vesicle endocytosis. *Curr. Opin. Neurobiol*. 10:312–320.

Cao, H., F. Garcia, and M.A. McNiven. 1998. Differential distribution of dynamin isoforms in mammalian cells. *Mol. Biol. Cell*. 9:2595–2609.

Clark, S.G., M.J. Stern, and H.R. Horvitz. 1992. *C. elegans* cell-signaling gene *sem-5* encodes a protein with SH2 and SH3 domains. *Nature*. 356:340–344.

Damke, H., T. Baba, D.E. Warnock, and S.L. Schmid. 1994. Induction of mutant dynamin specifically blocks endocytic coated vesicle formation. *J. Cell Biol*. 127:915–934.

de la Roche, M., and G.P. Cote. 1999. Characterization of a dyctiostelium homolog of yeast ABP1 that interacts with the N-terminus of myosin I heavy chain kinase. *Mol. Biol. Cell.* 10:165a. (Abstr.)

Drubin, D.G., K.G. Miller, and D. Botstein. 1988. Yeast actin-binding proteins: evidence for a role in morphogenesis. *J. Cell Biol.* 107:2551–2561.

Ellis, S., and H. Mellor. 2000. Regulation of endocytic traffic by rho family GTPases. *Trends Cell Biol*. 10:85–88.

Engqvist-Goldstein, Å.E.Y., M.M. Kessels, V.S. Chopra, M.R. Hayden, and D.G. Drubin. 1999. An actin-binding protein of the Sla2/Huntingtin interacting protein 1 family is a novel component of clathrin-coated pits and vesicles. *J. Cell Biol*. 147:1503–1518.

Ensenat, D., Z. Yao, X.S. Wang, R. Kori, G. Zhou, S.C. Lee, and T.-H. Tan. 1999. A novel src homology 3 domain-containing adaptor protein, HIP-55, that interacts with hematopoietic progenitor kinase 1. *J. Biol. Chem*. 274: 33945–33950.

Frischknecht, F., V. Moreau, S. Röttger, S. Gonfloni, I. Reckmann, G. Superti-Furga, and M. Way. 1999. Actin-based motility of vaccinia virus mimics receptor tyrosine kinase signalling. *Nature*. 401:926–929.

Fujimoto, L.M., R. Roth, J.E. Heuser, and S.L. Schmid. 2000. Actin assembly plays a variable, but not obligatory role in receptor-mediated endocytosis in mammalian cells. *Traffic*. 1:161–171.

Gaidarov, I., F. Santini, R.A. Warren, and J.H. Keen. 1999. Spatial control of coated-pit dynamics in living cells. *Nat. Cell Biol*. 1:1–7.

Geli, M.I., and H. Riezman. 1998. Endocytic internalization in yeast and animal cells: similar and different. *J. Cell Sci*. 111:1031–1037.

Goode, B.L., A.A. Rodal, G. Barnes, and D.G. Drubin. 2000. Reconstitution of actin assembly in *Saccharomyces cerevisiae* extracts and identification of new regulators of the Arp2/3 complex. *Mol. Biol. Cell.* 11:378a. (Abstr.)

Goslin, K., and G. Banker. 1991. Rat hippocampal neurons in low-density culture. *In* Culturing Nerve Cells. G. Banker and K. Goslin, editors. MIT Press, Cambridge, MA. 251–281.

Gout, I., R. Dhand, I.D. Hiles, M.J. Fry, G. Panayotou, P. Das, O. Truong, N.F. Totty, J. Hsuan, G.W. Booker, et al. 1993. The GTPase dynamin binds to and is activated by a subset of SH3 domains. *Cell*. 75:25–36.

Hilfiker, S., V.A. Pieribone, A.J. Czernik, H.-T. Kao, G.J. Augustine, and P. Greengard. 1999. Synapsins as regulators of neurotransmitter release. *Philos. Trans. R. Soc. Lond. B Biol. Sci*. 354:269–279.

Holtzman, D.A., S. Yang, and D.G. Drubin. 1993. Synthetic-lethal interactions identify two novel genes, SLA1 and SLA2, that control membrane cytoskeleton assembly in *Saccharomyces cerevisiae*. *J. Cell Biol.* 122:635–644.

Kessels, M.M., Å.E.Y. Engqvist-Goldstein, and D.G. Drubin. 2000. Association of mouse actin-binding protein 1 (mAbp1/SH3P7), an Src kinase target, with dynamic regions of the cortical actin cytoskeleton in response to Rac1 activation. *Mol. Biol. Cell*. 11:393–412.

Lappalainen, P., M.M. Kessels, M.J.T.V. Cope, and D.G. Drubin. 1998. The ADF homology (ADF-H) domain: a highly exploited actin-binding module. *Mol. Biol. Cell*. 9:1951–1959.

Larbolette, O., B. Wollscheid, J. Schweikert, P.J. Nielsen, and J. Wienands. 1999. SH3P7 is a cytoskeleton adapter protein and is coupled to signal transduction from lymphocyte antigen receptors. *Mol. Cell. Biol*. 19:1539–1546.

Lila, T., and D.G. Drubin. 1997. Evidence for physical and functional interactions among two *Saccharomyces cerevisiae* SH3 domain proteins, an adenylyl cyclase-associated protein and the actin cytoskeleton. *Mol. Biol. Cell*. 8:367–385.

Lock, P., C.L. Abram, T. Gibson, and S.A. Courtneidge. 1998. A new method for isolating tyrosine kinase substrates used to identify Fish, an SH3 and PX domain-containing protein, and Src substrate. *EMBO (Eur. Mol. Biol. Organ.) J*. 17:4346–4357.

Man, Y.-H., J.W. Lin, W.H. Ju, G. Ahmadian, L. Liu, L.E. Becker, M. Sheng, and Y.T. Wang. 2000. Regulation of AMPA receptor-mediated synaptic transmission by clathrin-dependent receptor internalization. *Neuron*. 25: 649–662.

Matus, A., M. Ackerman, G. Pehling, H.R. Byers, and K. Fujiwara. 1982. High actin concentration in brain dendritic spines and postsynaptic densities. *Proc. Natl. Acad. Sci. USA*. 79:7590–7594.

McNiven, M., H. Cao, K.R. Pitts, and Y. Yoon. 2000. The dynamin family of mechanoenzymes: pinching in new places. *Trends Cell Biol.* 25:115–120.

McPherson, P.S., K. Takei, S.L. Schmid, and P. De Camilli. 1994. p145, a major Grb2-binding protein in brain, is co-localized with dynamin in nerve terminals where it undergoes activity-dependent dephosphorylation. *J. Biol. Chem*. 269:30132–30139.

Merrifield, C.J., S.E. Moss, C. Ballestrem, B.A. Imhof, G. Giese, I. Wunderlich, and W. Almers. 1999. Endocytic vesicles move at the tips of actin tails in cultured mast cells. *Nat. Cell. Biol*. 1:72–74.

Micheva, K.D., B.K. Kay, and P.S. McPherson. 1997. Synaptojanin forms two separate complexes in the nerve terminal. Interactions with endophilin and amphiphysin. *J. Biol. Chem*. 272:27239–27245.

Napolitano, M., G.A. Marfia, A. Vacca, D. Centonze, D. Bellavia, L. Di Marcotullio, L. Frati, G. Bernardi, A. Gulino, and P. Calabresi. 1999. Modulation of gene expression following long-term synaptic depression in the striatum. *Brain Res. Mol. Brain Res*. 72:89–96.

Ochoa, G.C., V.I. Slepnev, L. Neff, N. Ringstad, K. Takei, L. Daniell, W. Kim, H. Cao, M. McNiven, R. Baron, and P. De Camilli. 2000. A functional link between dynamin and the actin cytoskeleton at podosomes. *J. Cell Biol*. 150: 377–390.

Qualmann, B., and R.B. Kelly. 2000. Syndapin isoforms participate in receptor-mediated endocytosis and actin organization. *J. Cell Biol*. 148:1047–1061.

Qualmann, B., J. Roos, P.J. DiGregorio, and R.B. Kelly. 1999. Syndapin I, a synaptic dynamin-binding protein that associates with the neural Wiskott-Aldrich syndrome protein. *Mol. Biol. Cell*. 10:501–513.

Qualmann, B., M.M. Kessels, and R.B. Kelly. 2000. Molecular links between endocytosis and the actin cytoskeleton. *J. Cell Biol.* 150:111–116.

Raths, S., J. Rohrer, F. Causaz, and H. Riezman. 1993. End3 and end4: two mutations defective in receptor-mediated and fluid-phase endocytosis in *Saccharomyces cerevisiae*. *J. Cell Biol.* 120:55–65.

Ringstad, N., Y. Nemoto, and P. De Camilli. 1997. The SH3p4/Sh3p8/SH3p13 protein family: binding partners for synaptojanin and dynamin via a Grb2-like Src homology 3 domain. *Proc. Natl. Acad. Sci. USA*. 94:8569–8574.

Roos, J., and R.B. Kelly. 1998. Dap160, a neural-specific Eps15 homology and multiple SH3 domain-containing protein that interacts with *Drosophila* dynamin. *J. Biol. Chem*. 273:19108–19119.

Roos, J., and R.B. Kelly. 1999. The endocytic machinery in nerve terminals surrounds sites of exocytosis. *Curr. Biol*. 9:1411–1414.

Rozelle, A.L., L.M. Machesky, M. Yamamoto, M.H.E. Driessens, R.H. Insall, M.G. Roth, K. Luby-Phelps, G. Marriott, A. Hall, and H.L. Yin. 2000. Phosphatidylinositol 4,5-bisphosphate induces actin-based movement of raft-enriched vesicles through WASP-Arp2/3. *Curr. Biol*. 10:311–320.

Scaife, R., I. Gout, M.D. Waterfield, and R.L. Margolis. 1994. Growth factor-induced binding of dynamin to signal transduction proteins involves sorting to distinct and separate proline-rich dynamin sequences. *EMBO (Eur. Mol. Biol. Organ.) J*. 13:2574–2582.

Sever, S., H. Damke, and S.L. Schmid. 2000. Garrotes, springs, ratchets, and whips: putting dynamin models to the test. *Traffic*. 1:385–392.
Simpson, F., N.K. Hussain, B. Qualmann, R.B. Kelly, B.K. Kay, P.S. McPherson, and S.L. Schmid. 1999. SH3-domain-containing proteins function at distinct steps in clathrin-coated vesicle formation. *Nat. Cell. Biol*. 1:119–124.
Sparks, A.B., N.G. Hoffman, S.J. McConnell, D.M. Fowlkes, and B.K. Kay. 1996. Cloning of ligand targets: systematic isolation of SH3 domain-containing proteins. *Nat. Biotechnol*. 14:741–744.
Takei, K., P.S. McPherson, S.L. Schmid, and P. De Camilli. 1995. Tubular membrane invaginations coated by dynamin rings are induced by GTP-gamma S in nerve terminals. *Nature.* 374:186–190.
Taunton, J., B.A. Rowning, M.L. Coughlin, M. Wu, R.T. Moon, T.J. Mitchison, and C.A. Larabell. 2000. Actin-dependent propulsion of endosomes and lysosomes by recruitment of N-WASP. *J. Cell Biol.* 148:519–530.
Tebar, F., A. Soprkina, A. Sorkin, M. Ericsson, and T. Kirchausen. 1996. Eps15 is a component of clathrin-coated pits and vesicles and is located at the rim of coated pits. *J. Biol. Chem.* 271:28727–28730.
Ware, M.F., D.A. Tice, S.J. Parsons, and D.A. Lauffenburger. 1997. Overexpression of cellular Src in fibroblasts enhances endocytic internalization of epidermal growth factor receptor. *J. Biol. Chem*. 272:30185–30190.
Wendland, B., S.D. Emr, and H. Riezman. 1998. Protein traffic in the yeast endocytic and vacuolar protein sorting pathways. *Curr. Opin. Cell Biol*. 10:513–522.
Wesp, A., L. Hicke, J. Palecek, R. Lombardi, T. Aust, A.L. Munn, and H. Riezman. 1997. End4p/S1a2p interacts with actin-associated proteins for endocytosis in *Saccharomyces cerevisiae*. *Mol. Biol. Cell*. 8:2291–2306.
Wigge, P., and H.T. McMahon. 1998. The amphiphysin family of proteins and their role in endocytosis at the synapse. *Trends Neurosci*. 21:339–344.
Wigge, P., Y. Vallis, and H.T. McMahon. 1997. Inhibition of receptor-mediated endocytosis by the amphiphysin SH3 domain. *Curr. Biol.* 7:554–560.
Wilde, A., E.C. Beattie, L. Lem, D.A. Riethof, S.-H. Liu, W.C. Mobley, P. Soriano, and F.M. Brodsky. 1999. EGF receptor signaling stimulates SRC kinase phosphorylation of clathrin, influencing clathrin redistribution and EGF uptake. *Cell*. 96:677–687.
Witke, W., A.V. Podtelejnikov, A. Di Nardo, J.D. Sutherland, C.B. Gurniak, C. Dotti, and M. Mann. 1998. In mouse brain profilin I and profilin II associate with regulators of the endocytic pathway and actin assembly. *EMBO (Eur. Mol. Biol. Organ.) J*. 17:967–976.
Yamabhai, M., N.G. Hoffman, N.L. Hardison, P.S. McPherson, L. Castagnoli, G. Cesareni, and B.K. Kay. 1998. Intersectin, a novel adaptor protein with two Eps15 homology and five Src homology 3 domains. *J. Biol. Chem*. 273: 31401–31407.